2. ANALYSIS OF NOISE/INTERFERENCE DATA

2.1 Description of Data

As part of its experimental wideband HF communications program, the Mitre Corporation has made recordings of wideband HF noise/interference. These data were obtained using a wideband HF communications test facility, which includes a simplex link from Homestead, FL to Bedford, MA.

The equipment used in the experiments is described by Perry and Rifkin (1989). Briefly, the communications system uses a direct sequence spread spectrum signal with a chipping rate of 512 kb/s. At the receive terminal a horizontally polarized log-periodic antenna (H/LPA) was used when the data in this report were obtained. The H/LPA has a directivity of about 10 dBi.

The wideband receiver converts the signal from rf to baseband where the complex (in-phase and quadrature) components are low-pass filtered (bandwidth = 400 kHz) and digitized at a sampling rate of 1.024 MHz. These filters truncate the received signal spectrum to an equivalent rf bandwidth of 800 kHz. Eight-bit analog to digital converters were used. In addition, a variable attenuator (0-31 dB) was used at the receiver front-end to avoid saturating the receiver.

An important part of Mitre's wideband HF test facility is a frequency-domain interference suppressor which excises narrowband interference above a chosen threshold. However, the data discussed in this report are raw data that were obtained prior to interference excision.

The data consist of 42 one-second records of the digitized, baseband in-phase (I) and quadrature (Q) components of the received noise/interference. The data were collected during experiments performed in March, 1989 in Bedford, MA at various times of day and at various frequencies in the HF band (3-30 MHz). The times, dates, and center frequencies of the data, and the values of the variable attenuation that were used are listed in Table 1 of the Appendix. Also shown in the Appendix are example plots of the raw data (both I and Q). Each plot shows the first 4 ms (4096 samples) of a one-second noise/interference record.

The fact that the noise/interference is characterized by baseband I and Q components, whose bandwidth is less than the carrier frequency, implies that the noise/interference can be viewed as a narrowband process with a well-defined envelope and phase. However, the noise/interference is referred to as "wideband" in the sense that one is dealing with bandwidths on the order of 1 MHz as opposed to bandwidths on the order of several kHz.

2.2 Analysis Tools

To analyze the noise/interference data, software has been developed to generate the following quantities:

- plots of raw data (I and Q)
- probability density function (pdf) of raw data
- pdf of voltage envelope $\sqrt{(I^2 + Q^2)}$
- pdf of power envelope $(I^2 + Q^2)$
- pdf of phase $(\tan^{-1} Q/I)$
- cumulative distribution function (cdf) of power envelope
- distribution of average level crossing rate of the voltage envelope
- autocorrelation function of raw data
- power spectrum
- cdf of power in the frequency domain (sum of the squares of the real and imaginary parts of the complex Fourier transform of the raw data)
- pdf of phase in the frequency domain (phase of the complex Fourier transform of the raw data)

In addition, software has been developed to perform the following functions:

- frequency domain excision of narrowband interference
- simulations of noise/interference

The purpose of generating the rather large number of quantities listed above is to examine the noise/interference from many points of view simultaneously. This is necessary,

because, as discussed above, the objective of the present effort is not simply to model certain statistical characteristics of the noise/interference, but to obtain a model of the noise/interference process itself. Nevertheless, it may be noted that taken together, these quantities contain some redundancy. For example, the cdf of the power envelope is the integral of the pdf of the power envelope, and the latter quantity is related to the pdf of the voltage envelope through a simple transformation of variables. However, as will be seen in the examples below, certain characteristics of the noise/interference are sometimes more readily apparent in one quantity than in another which, in principle, contains the same information.

On the other hand, these quantities do not provide a complete characterization of the noise/interference. As was pointed out above, the higher-order statistics have not been examined in the present effort, although we intend to do so in future work.

2.3 Case Studies

The general strategy which has been used to analyze the noise/interference data is as follows. First, plots of the raw data, examples of which appear in the Appendix, were examined qualitatively to identify data which seemed typical of the total data set. Next, the data so identified was analyzed in detail with the intent of developing a simple physical model of the noise/interference capable of describing the data. Then the raw data was reexamined for examples which seemed qualitatively different from the typical case. Finally, these examples were analyzed to determine whether the tentative model could also describe these cases, and, if not, to determine how the model could be modified and/or extended to include these cases. Thus, a variety of case studies were conducted.

2.3.1 Case Study 1.

The data analyzed in this case study are typical of the wideband noise/interference records which have been examined. These data were obtained on 10 March 1989 at 9:58:10 UT at a center frequency of 5.936 MHz.

A plot of the first 4 ms of the I-channel data is shown in Figure 1. The pdf of these data is shown in Figure 2 in the form of a histogram, which resembles a Gaussian

distribution. This is not surprising, because over an 800 kHz bandwidth one expects contributions to the noise/interference from many independent sources, which, by the central limit theorem, may be expected to approximate a Gaussian process. If the noise/interference is a complex, zero-mean Gaussian process, the voltage envelope is Rayleigh distributed. Figure 3 shows the pdf of the voltage envelope, which does indeed resemble a Rayleigh distribution. The pdf of the phase is shown in Figure 4, and is approximately a uniform distribution, which again is expected if the I and Q data correspond to independent, identically distributed zero-mean Gaussian processes.

However, Figure 5, which shows the pdf of the power envelope, indicates that the noise/interference cannot adequately be described by a Gaussian process alone. Whereas the power envelope for a Gaussian process is exponentially distributed, the pdf in Figure 5 shows a pronounced dip for small values of power. In fact, the distribution resembles a Rician power distribution, which arises from one or more sine waves in the presence of Gaussian noise. Thus, it appears that the noise/interference can be described by a combination of Gaussian noise and narrowband interference (sine waves).

The cdf of the power envelope, plotted as the logarithm of the probability that the power exceeds some threshold as a function of the logarithm of that threshold, is shown in Figure 6. Although this function in principle contains the same information as the power pdf in Figure 5, log-log plots reveal the tails of probability distributions more clearly than linear plots. Examples of this effect can be seen in some of the case studies discussed below.

The level crossing distribution of the voltage envelope is shown in Figure 7. Plotted is the number of upgoing crossings (in a time interval of 4 ms) of the voltage envelope across a given threshold as a function of that threshold. Thus, the number of crossings divided by 4 ms gives the average level crossing rate in crossings per second. It can be shown that the average level crossing rate of the voltage envelope is proportional to the pdf of the voltage envelope for a Gaussian process (Rice, 1944 and 1945), but not for random processes in general (see, for example, Hall, 1966). However, comparing Figure 7 with

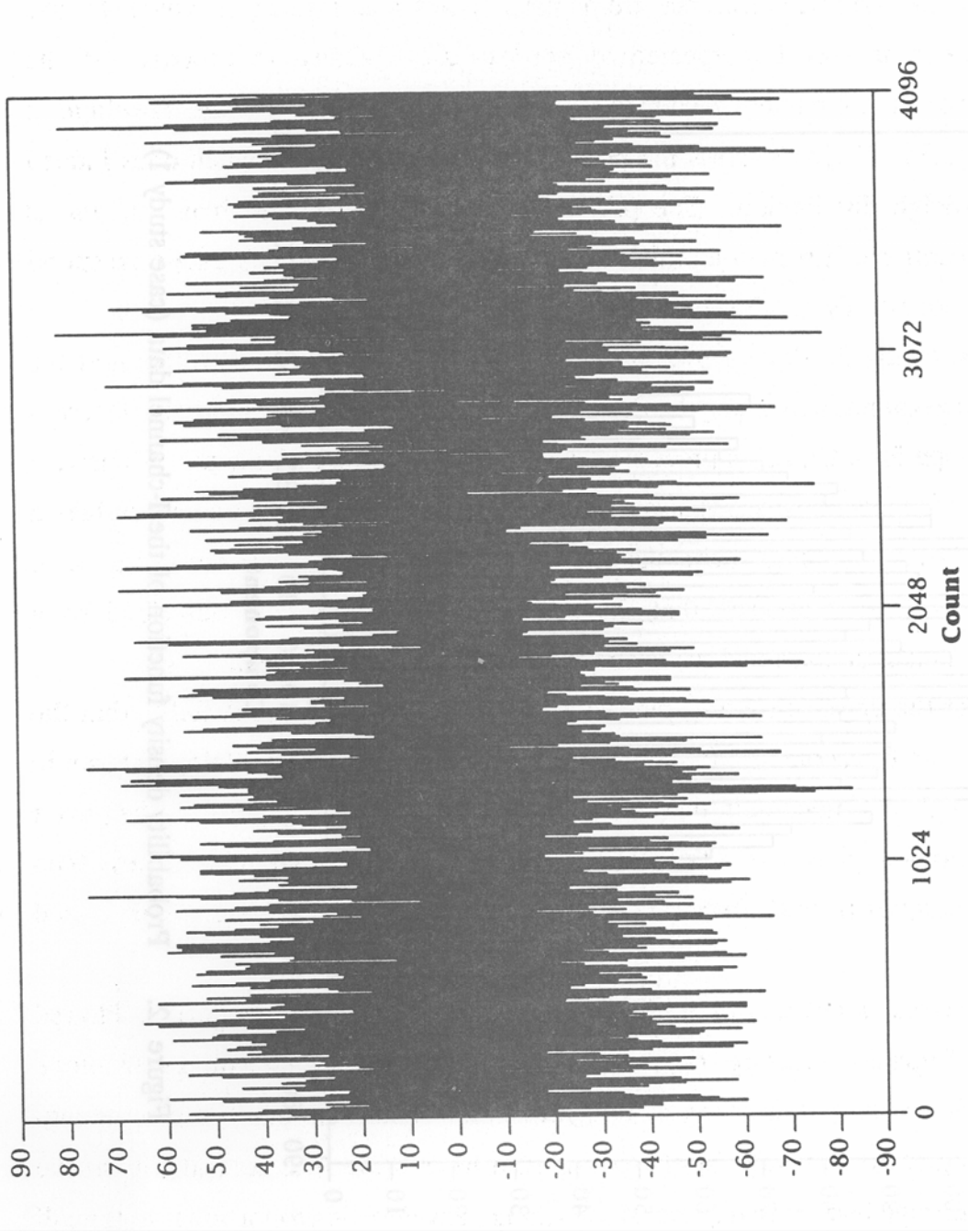

Figure 1. Measured noise/interference in the I-channel at 5.936 MHz (case study 1).

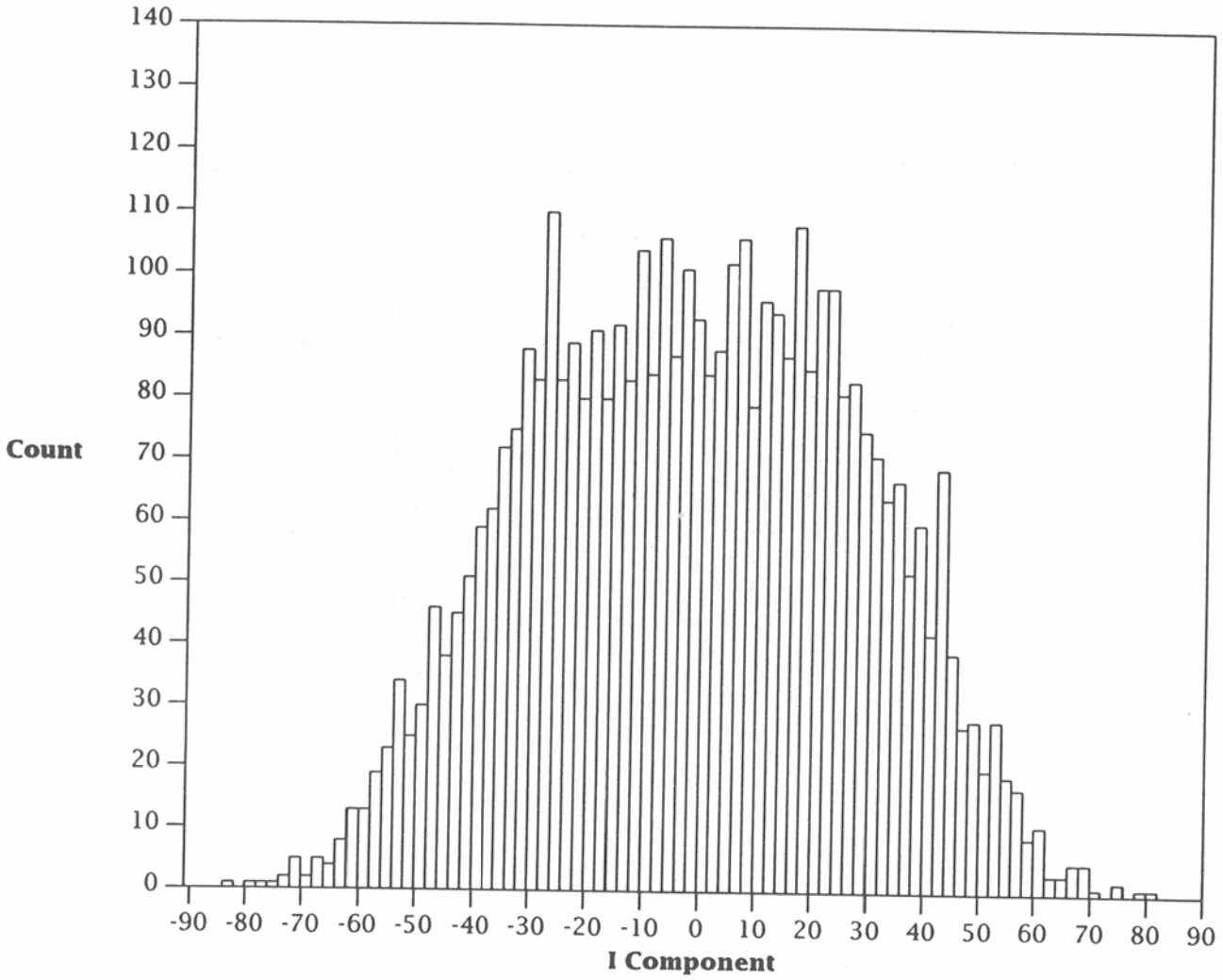

Figure 2. Probability density function of the I-channel data (case study 1).

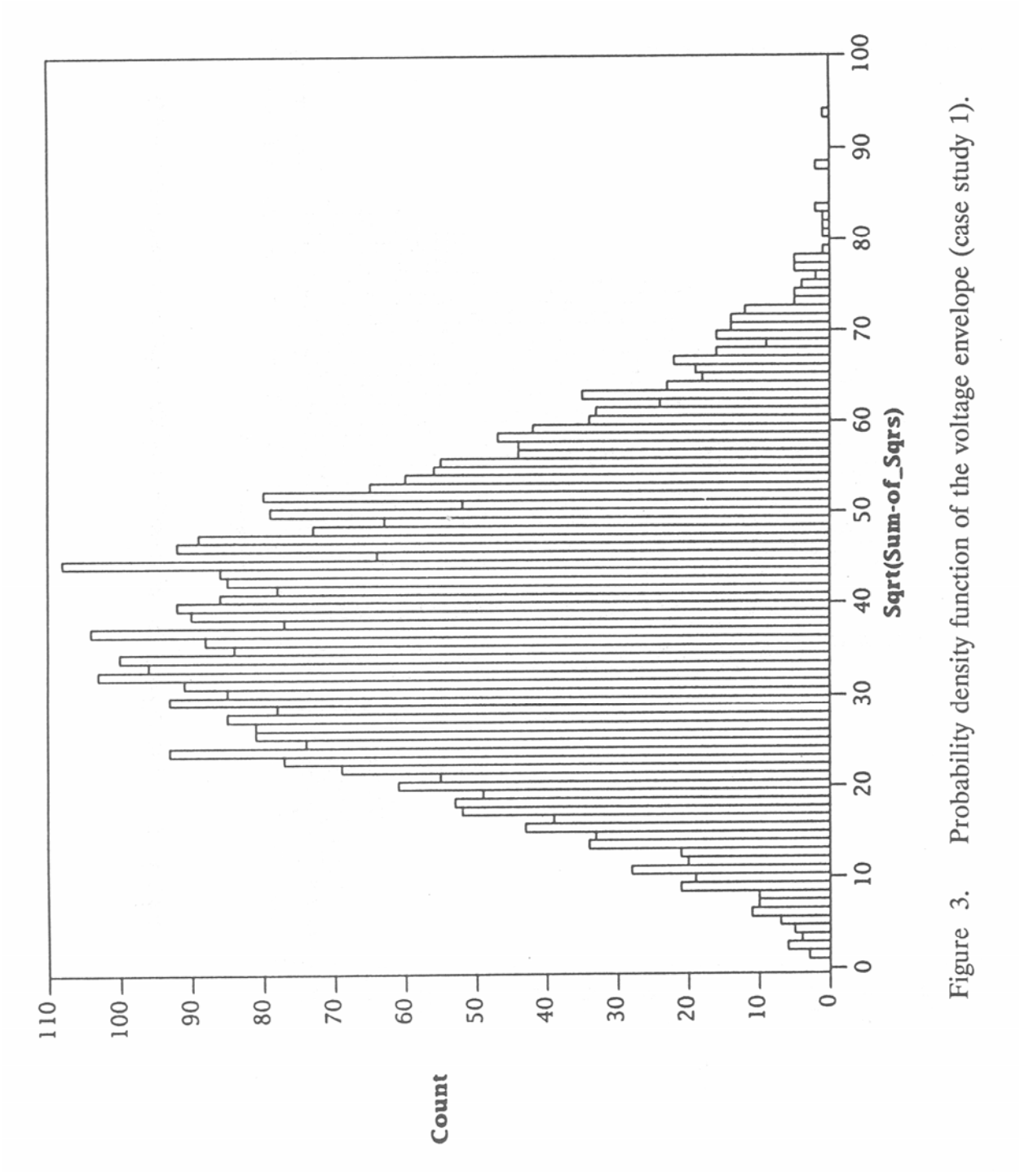

Figure 3. Probability density function of the voltage envelope (case study 1).

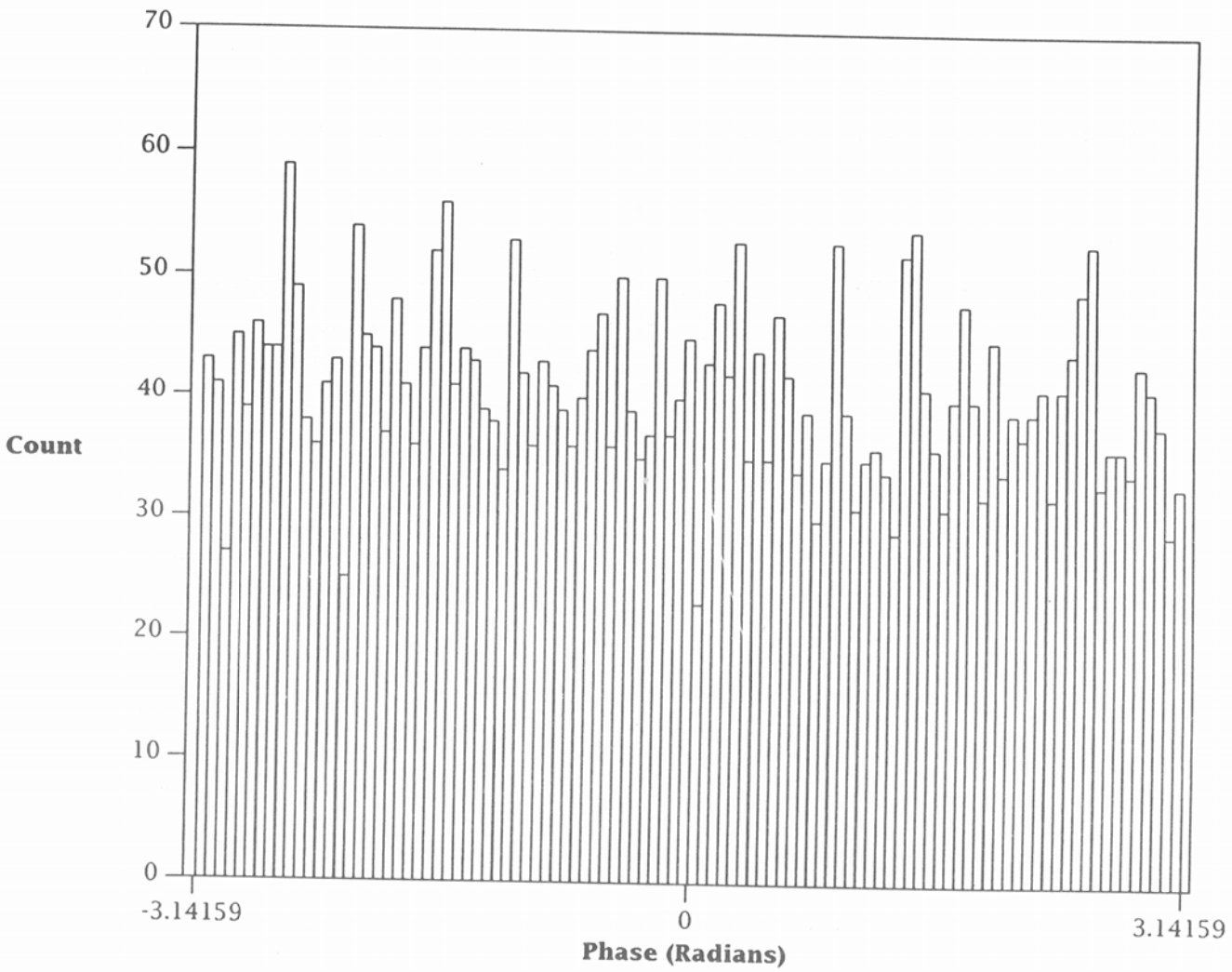

Figure 4. Probability density function of the phase (case study 1).

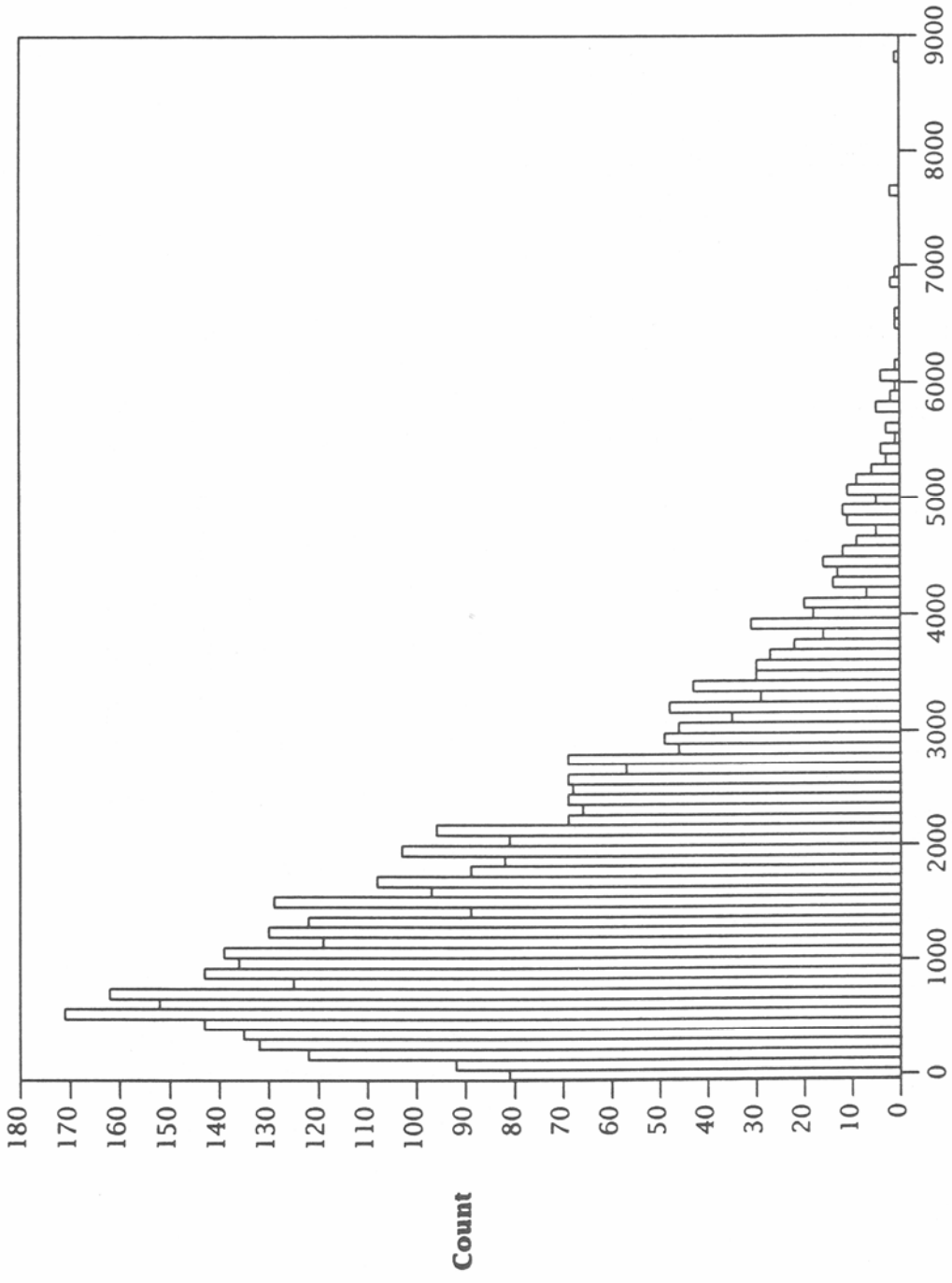

Figure 5. Probability density function of the power envelope (case study 1).

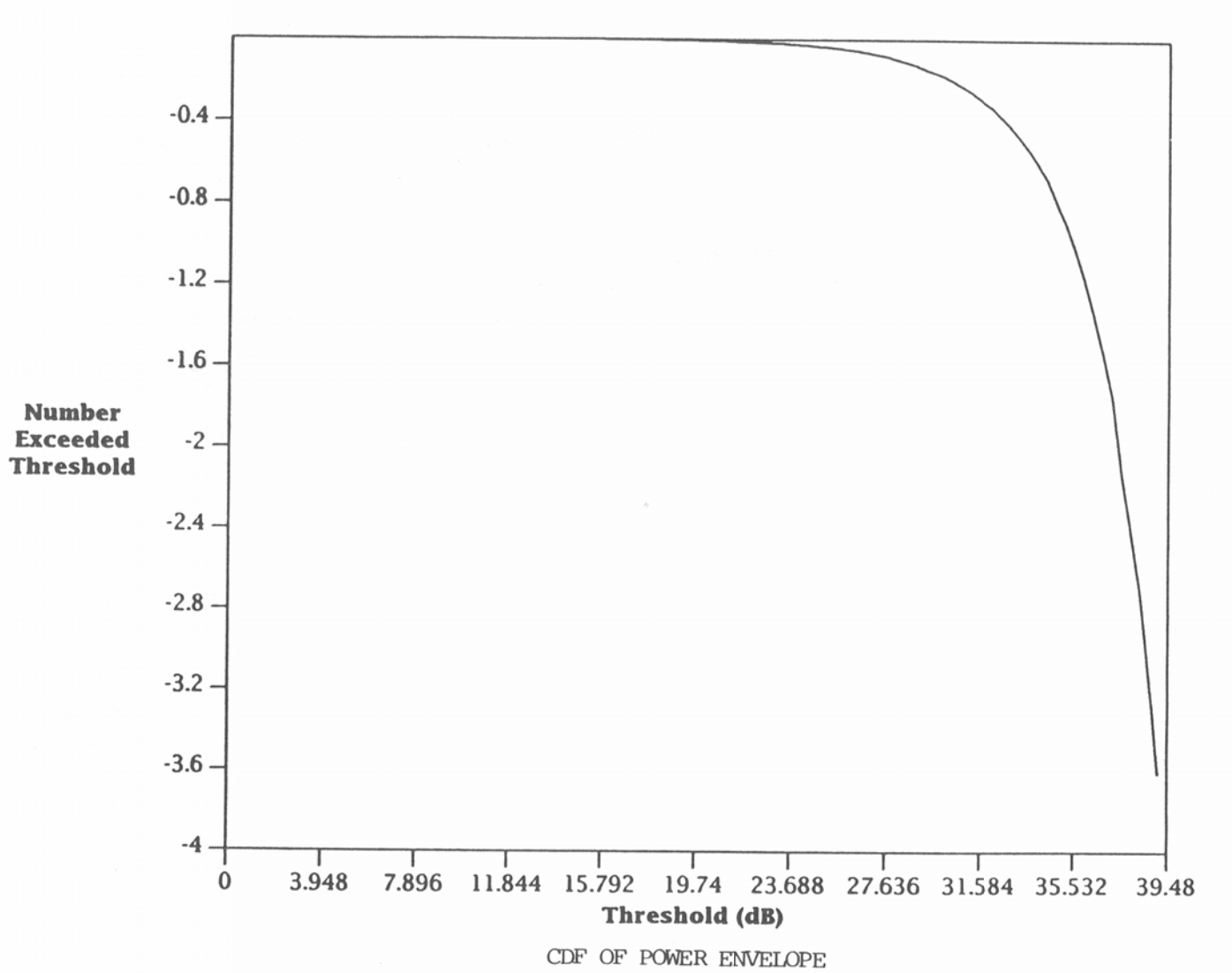

Figure 6. Cumulative distribution function of the power envelope (case study 1).

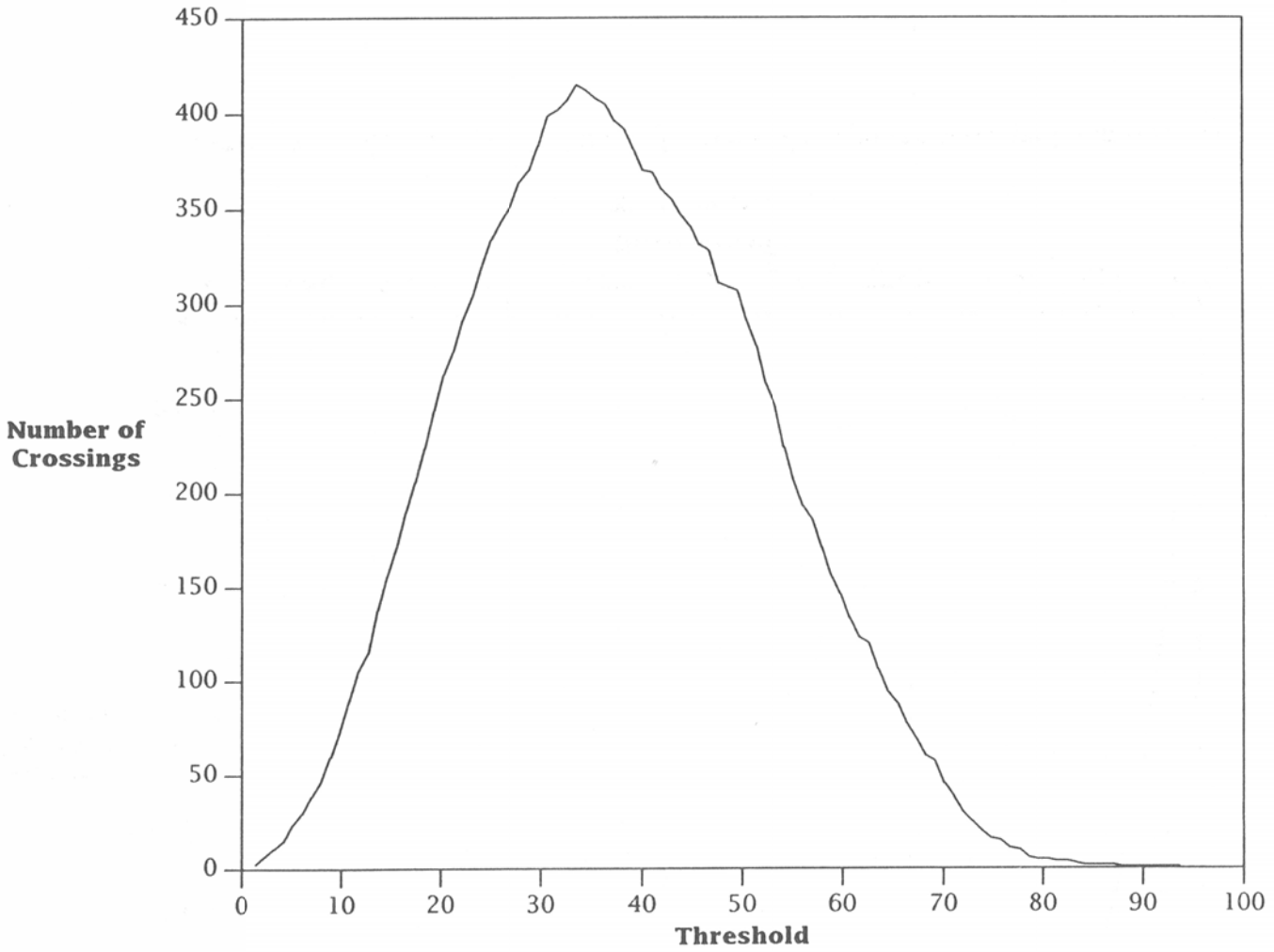

Figure 7. Level crossing distribution of the voltage envelope (case study 1).

Figure 3 (voltage envelope pdf) shows that the crossing rate is approximately proportional to the envelope pdf in this case.

The analyses discussed so far provide a description of the first-order statistics (average behavior of the envelope and phase) of the noise/interference in time. However, it remains to investigate the spectral properties of the process.

Figure 8 shows the power spectrum, obtained by computing the sum of the squares of the real and imaginary parts of the complex Fourier transform of the raw data. Because the transform is a discrete transform of a 4 ms record sampled at 1.024 MHz, the power spectrum spans a bandwidth of 1.024 MHz with a spectral resolution of 250 Hz. The spectrum has been folded so that the zero frequency at baseband (center frequency at rf) appears at the far left and right ends of the frequency scale. Also note that the power spectral density is plotted on a logarithmic (dB) scale.

The power spectrum clearly reveals the presence of many narrowband interferers. The absence of these interferers from the center of the plot is due to the fact that this part of the spectrum is outside the bandpass of the lowpass filter in the wideband receiver.

To characterize the amplitude distribution of the narrowband interferers, the cdf of the power envelope (sum of the squares of the real and imaginary parts) of the Fourier transform has been computed and is shown in Figure 9. As was done for the power cdf in the time domain (Figure 6), the logarithm of the probability that the power exceeds a threshold is plotted as a function of that threshold in dB. The form of the cdf in Figure 9 closely resembles analogous results obtained independently by Perry and Abraham (1988) and shown by Lemmon (1989) to be well described by a combination of a Gaussian process and an impulsive process defined by a model developed by Hall (1966). This observation has proved to be of considerable practical value in developing a noise/interference model because the Hall model involves simple analytical expressions.

Finally, the pdf of the phase of the Fourier transform is shown in Figure 10. Unlike the phase distribution in the time domain, the distribution in Figure 10 is clearly nonuniform.

To summarize, the results obtained thus far suggest that the noise/interference can be viewed as a combination of a Gaussian process and many narrowband interferers.

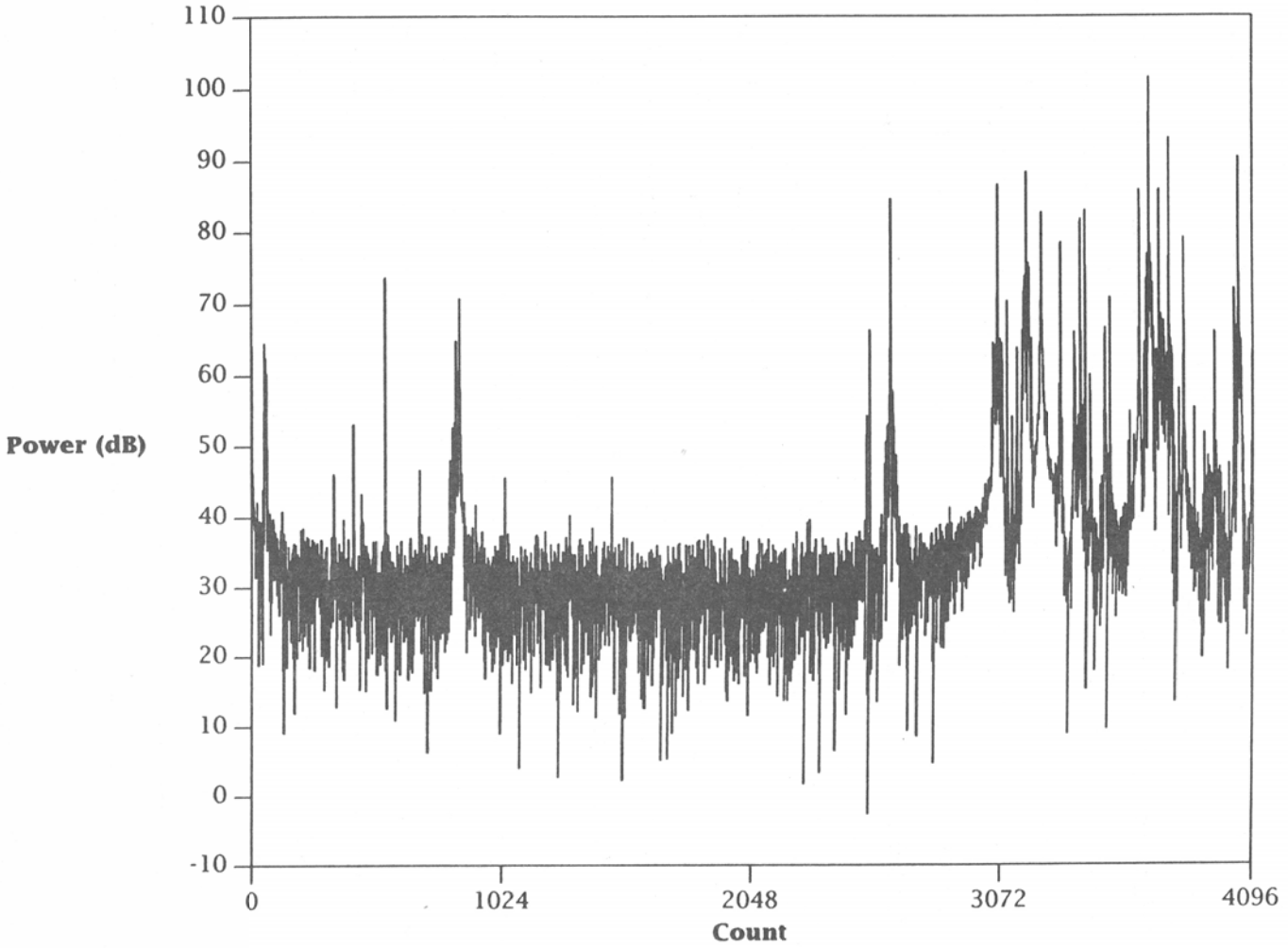

Figure 8. Power spectrum over a bandwidth of 1.024 MHz (case study 1).

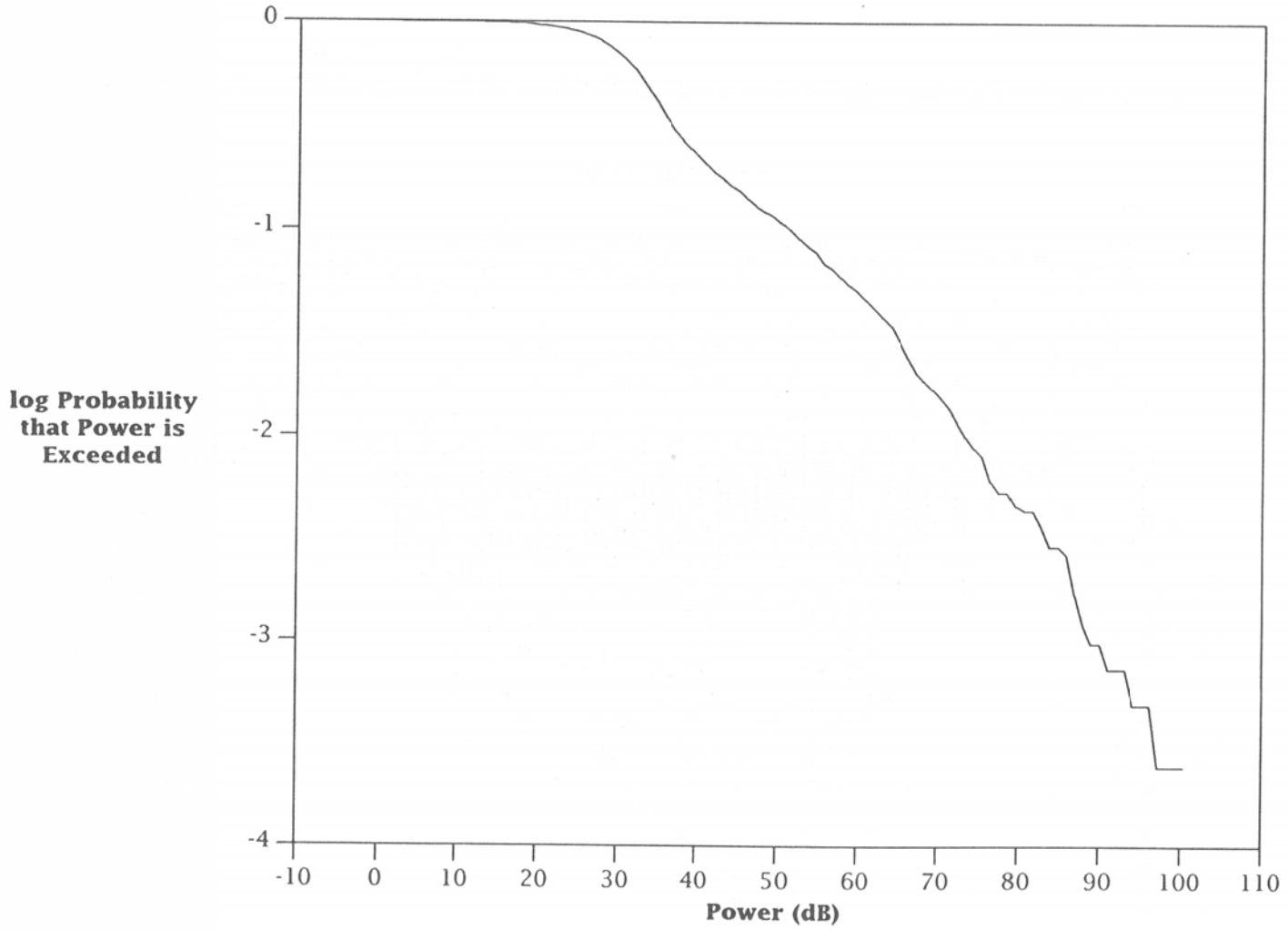

Figure 9. Cumulative distribution function of the power envelope in the frequency domain (case study 1).

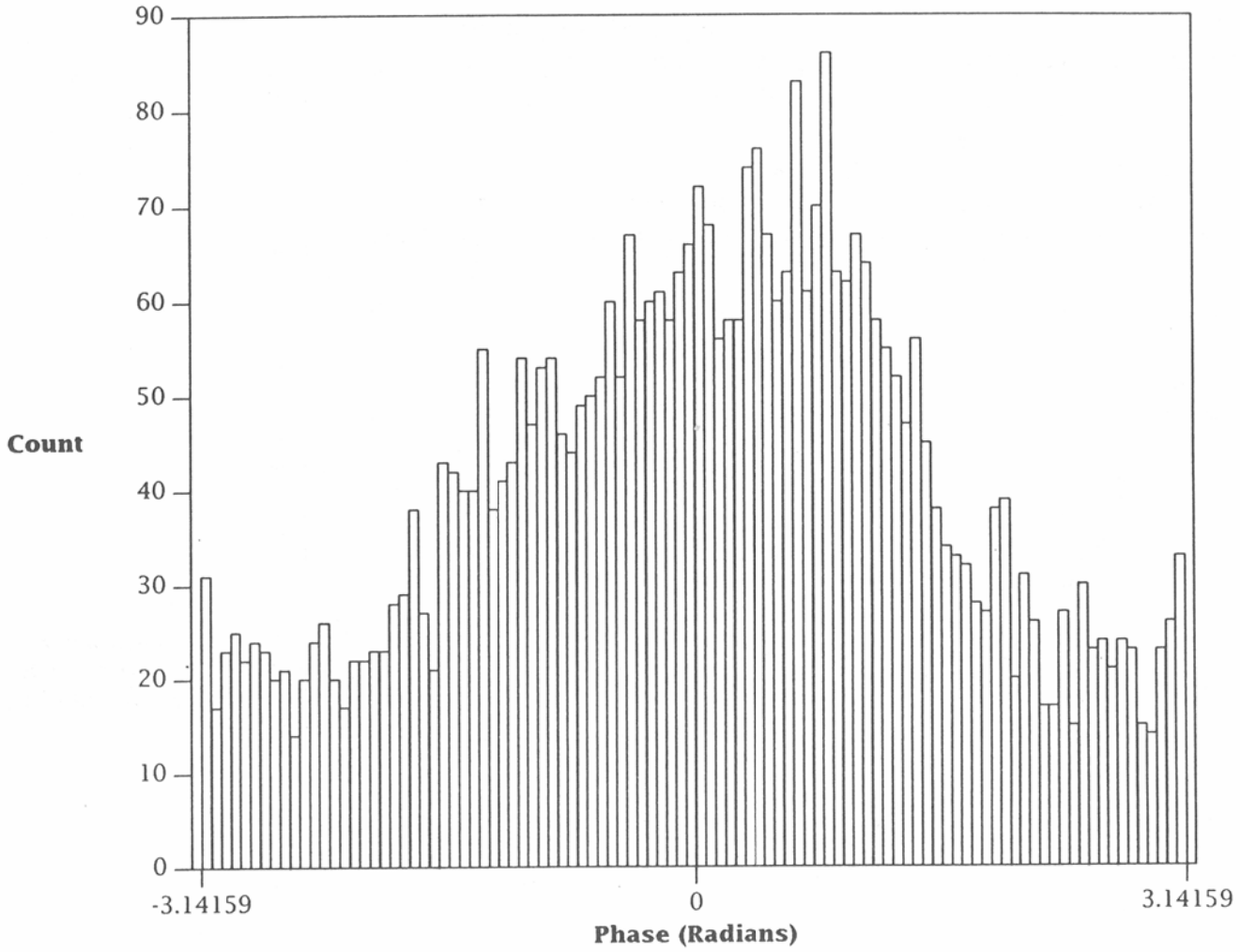

Figure 10. Probability density function of the phase in the frequency domain (case study 1).

2.3.2 Case Study 2.

This case study involves data that were obtained at 22:10:39 UT on 28 March 1989 at a center frequency of 19.29 MHz. A plot of the first 4 ms of the I-channel data is shown in Figure 11. This case was selected because the raw data shows a characteristic envelope modulation that is not present in most of the raw data records.

The pdf and the cdf of the power envelope in the time domain are shown in Figures 12 and 13, respectively. These distributions are qualitatively similar to the corresponding distributions in the previous case study, except that the pdf in the present case shows a more pronounced dip at small power levels. In terms of a Rician model (Gaussian noise combined with cw interferers), this simply means that the ratio of cw power to Gaussian power is greater in the present case.

It remains to explain the envelope modulation in the raw data. At first glance the modulation appears similar to the beating pattern resulting from the sum of two sine waves closely spaced in frequency, that is, a carrier at the average frequency, amplitude modulated by a sine wave of half the difference frequency. Note that modulation by a sine wave of half the difference frequency results in a beat frequency (number maxima of the envelope per unit time) equal to the frequency difference.

The power spectrum, shown in Figure 14, clearly reveals the presence of two strong narrowband interferers closely spaced in frequency, as well as a third, stronger interferer. However, the frequency difference between the two closely spaced interferers is approximately 8 kHz, whereas the beat frequency in the raw data is approximately 4 kHz. Moreover, a careful examination of the raw data shows that the positive voltage envelope does not coincide (in time) with the negative voltage envelope (as it does for the sum of two sine waves), but is displaced by one half cycle.

It can be shown, however, that the presence of a third sine wave, at the appropriate frequency, can indeed result in this type of pattern. To show that this is the case, one component of the spectral doublet was excised from the Fourier transform of the raw data, and the result was inverse Fourier transformed. The I-component of the resulting noise/interference is shown in Figure 15; the envelope modulation is clearly absent.

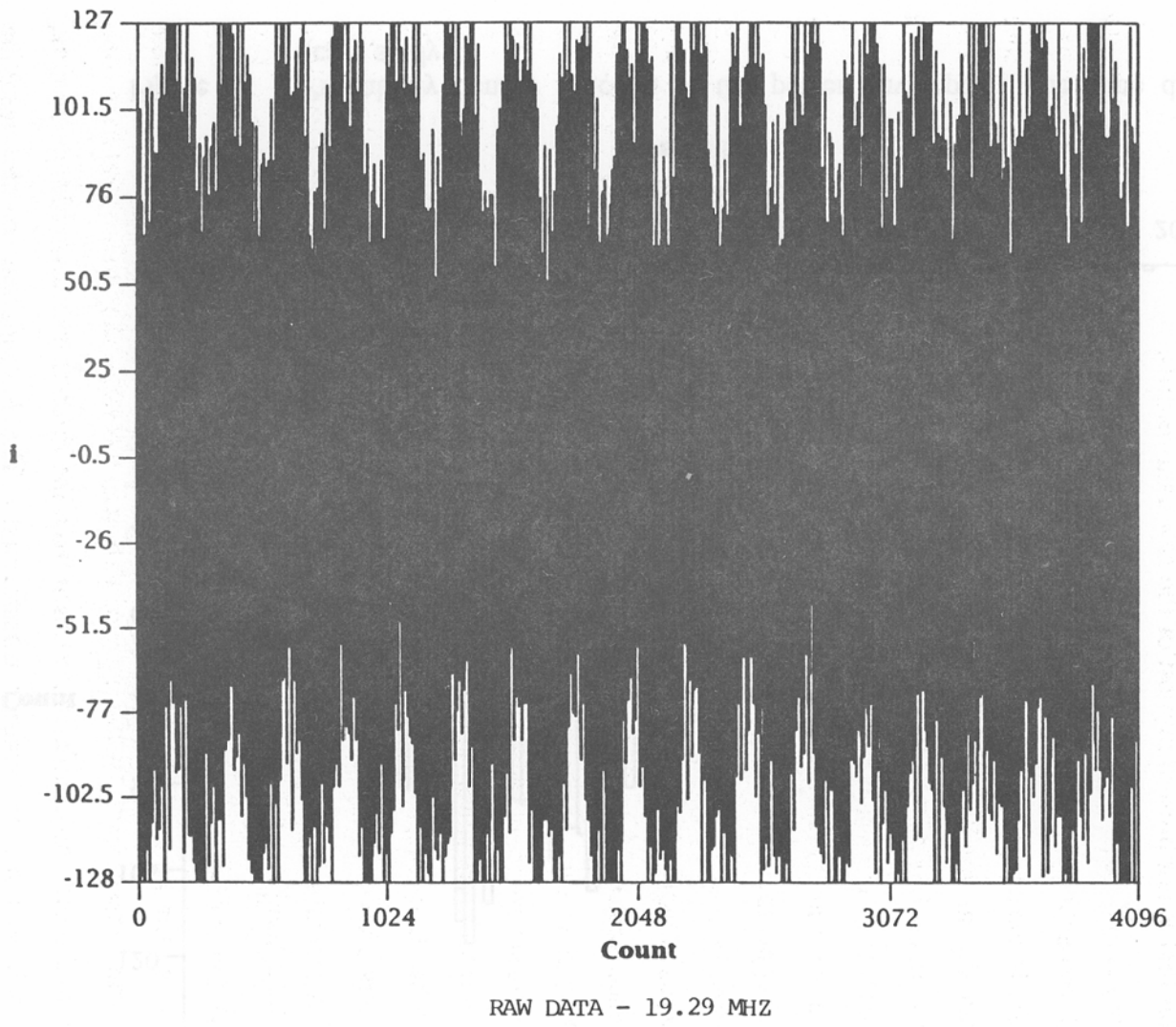

Figure 11. I-channel data at 19.29 MHz (case study 2).

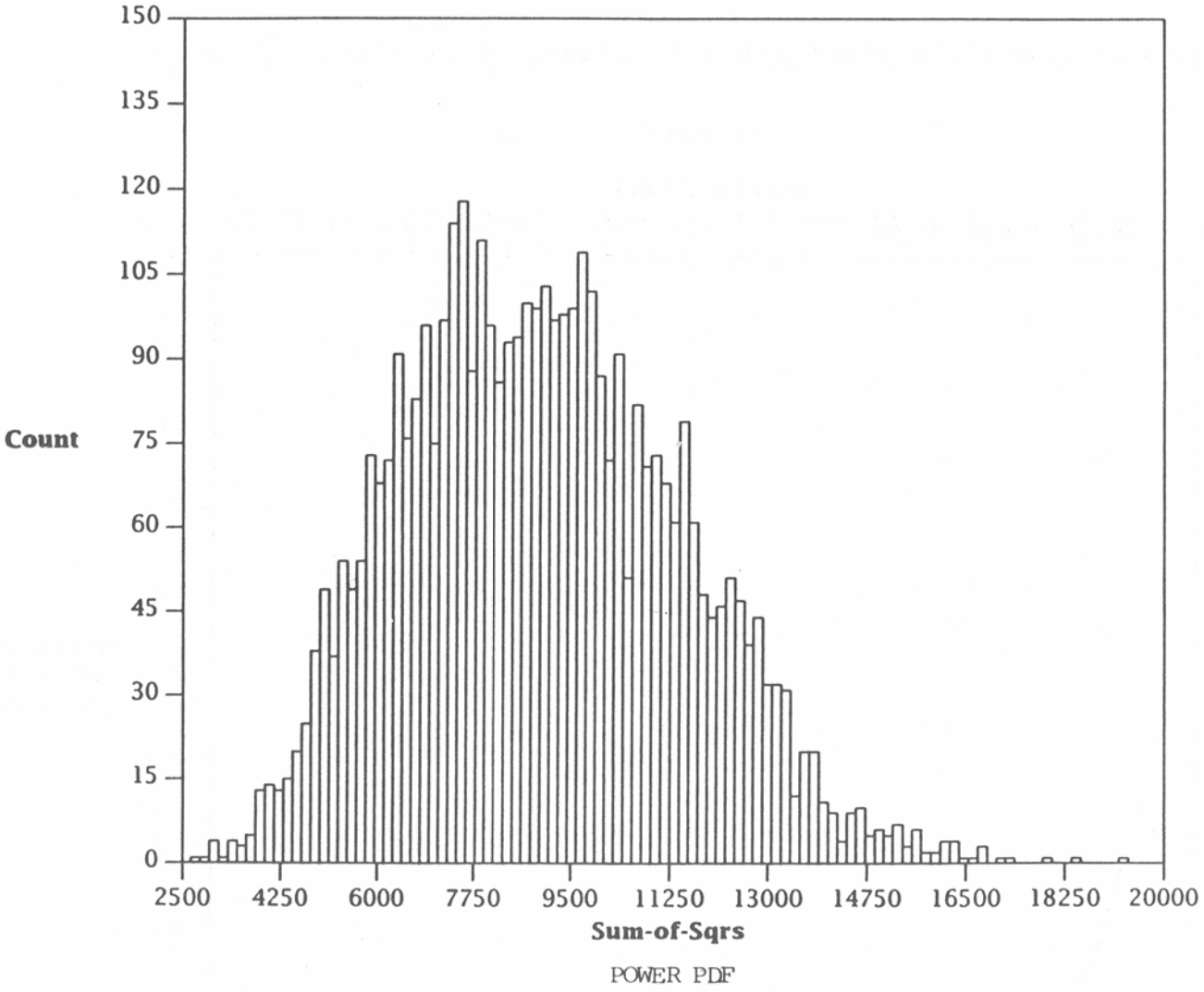

Figure 12. Probability density function of the power envelope in the time domain (case study 2).

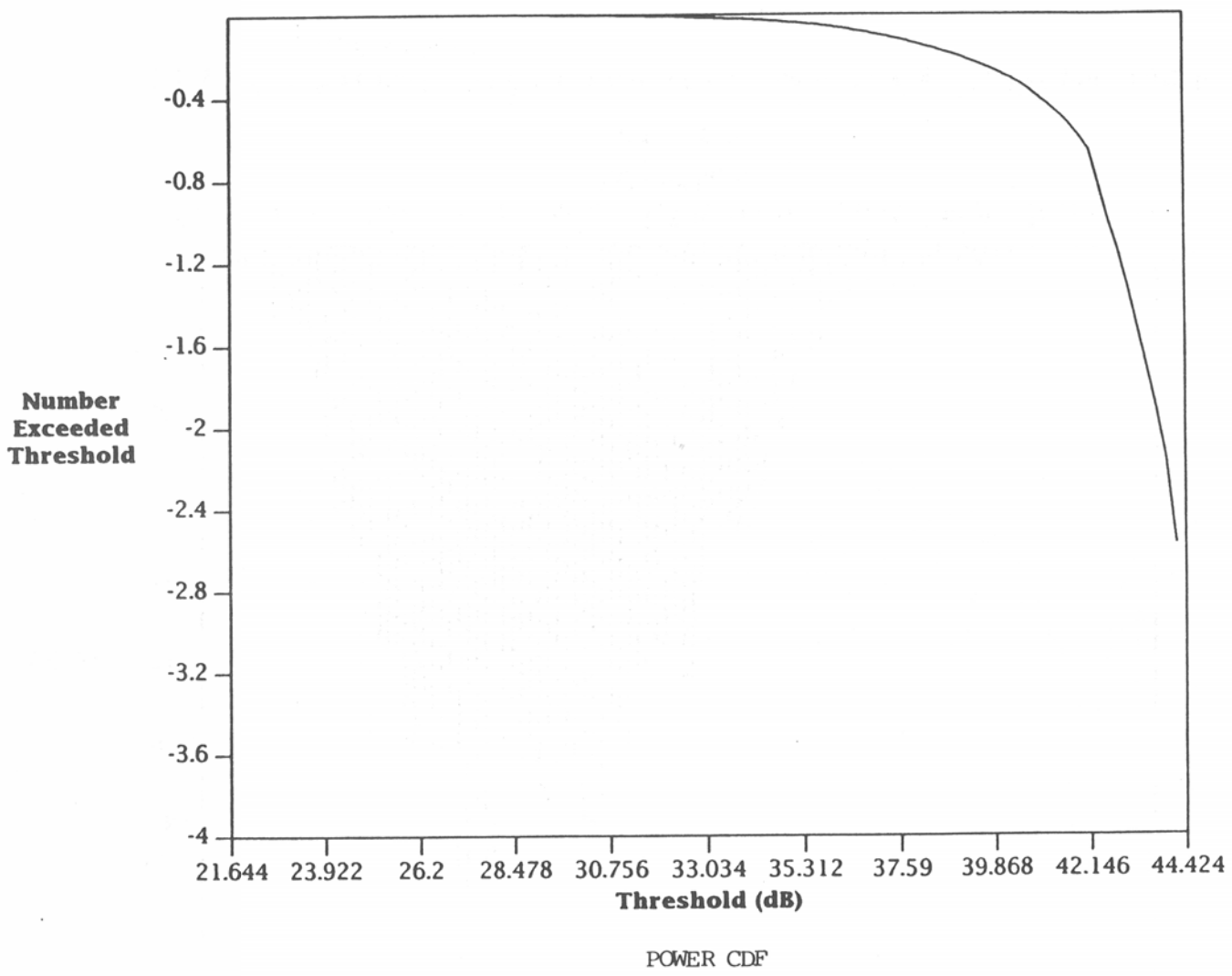

Figure 13. Cumulative distribution function of the power envelope in the time domain (case study 2).

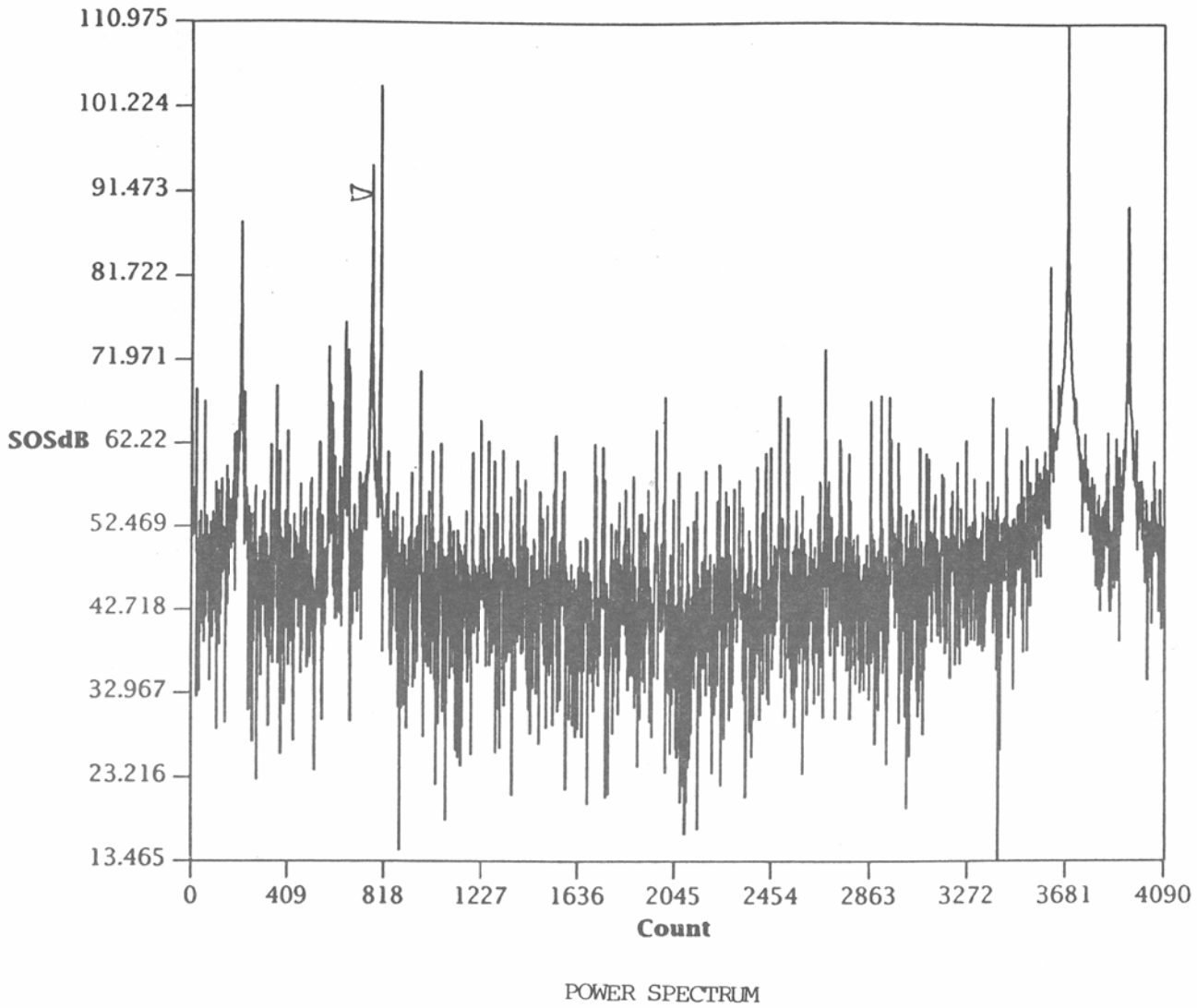

Figure 14. Power spectrum over a bandwidth of 1.024 MHz (case study 2).

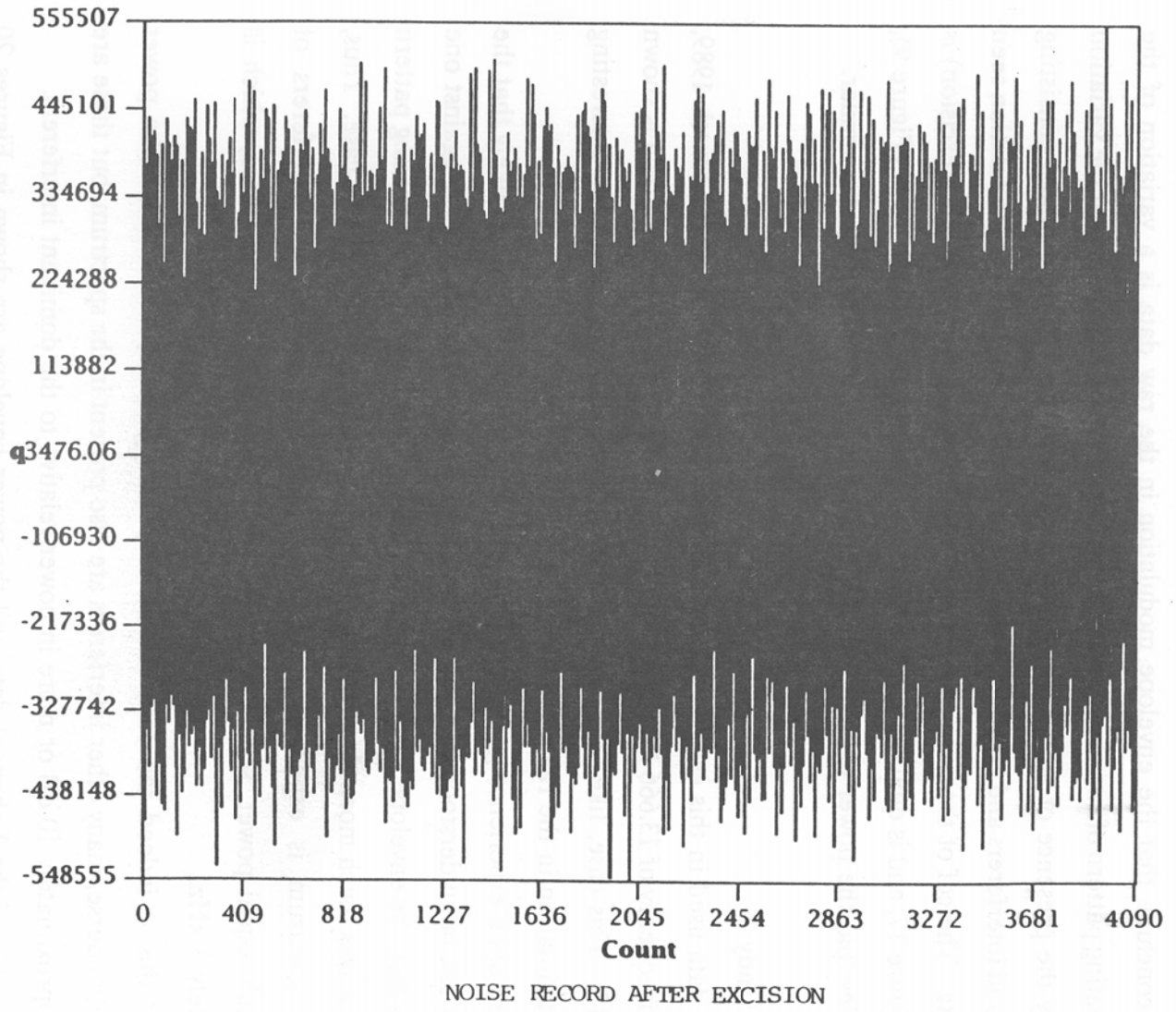

Figure 15. I-channel data after excision of a single narrowband interferer (case study 2).

It is also of interest to compare the pdf of the power envelope in the time domain after excision, shown in Figure 16, with the corresponding pdf before excision (Figure 12). The change in the shape of the pdf due to excision can be understood in terms of a Rician power distribution with a smaller ratio of cw power to Gaussian power.

We conclude that the envelope modulation in the raw data is a variation of the standard beating pattern of two closely spaced narrowband interferers, and that the variation is caused by the presence of additional narrowband interferers. Thus, a model consisting of narrowband interferers and Gaussian noise can account for the envelope modulation seen in these data. The cdf of the power envelope in the frequency domain (before excision) is shown in Figure 17, and is qualitatively similar to that in the previous case study (Figure 9), which implies that the power distribution of the narrowband interferers is also similar.

2.3.3 Case Study 3.

The data used in this case study were obtained at 10:26:47 UT on 28 March 1989, at a center frequency of 13.666 MHz. A plot of the first 4 ms of the I-channel data is shown in Figure 18. This case, like the previous case, was selected because of the interesting envelope modulation in the raw data.

Based upon experience gained from the previous case study, it seems likely that the modulation can be understood in terms of two narrowband interferers beating against one another. In fact, the envelope modulation in the present case resembles the beating pattern of two sine waves much more closely than does the modulation in the previous case. Thus, the power spectrum is expected to show two dominant narrowband interferers of approximately equal power, separated by the beat frequency in the raw data, which is approximately 3 kHz.

That this is indeed the case can be seen in Figure 19, which shows the power spectrum. Of course, many other interferers are also present in the spectrum, but these are down by approximately 10 dB or more in power relative to the dominant interferers.

The pdfs of the I-channel data and the power envelope are shown in Figures 20 and 21, respectively. These distributions resemble inverse power laws more closely than the corresponding pdfs in the previous case studies (the tails of Gaussian and Rician

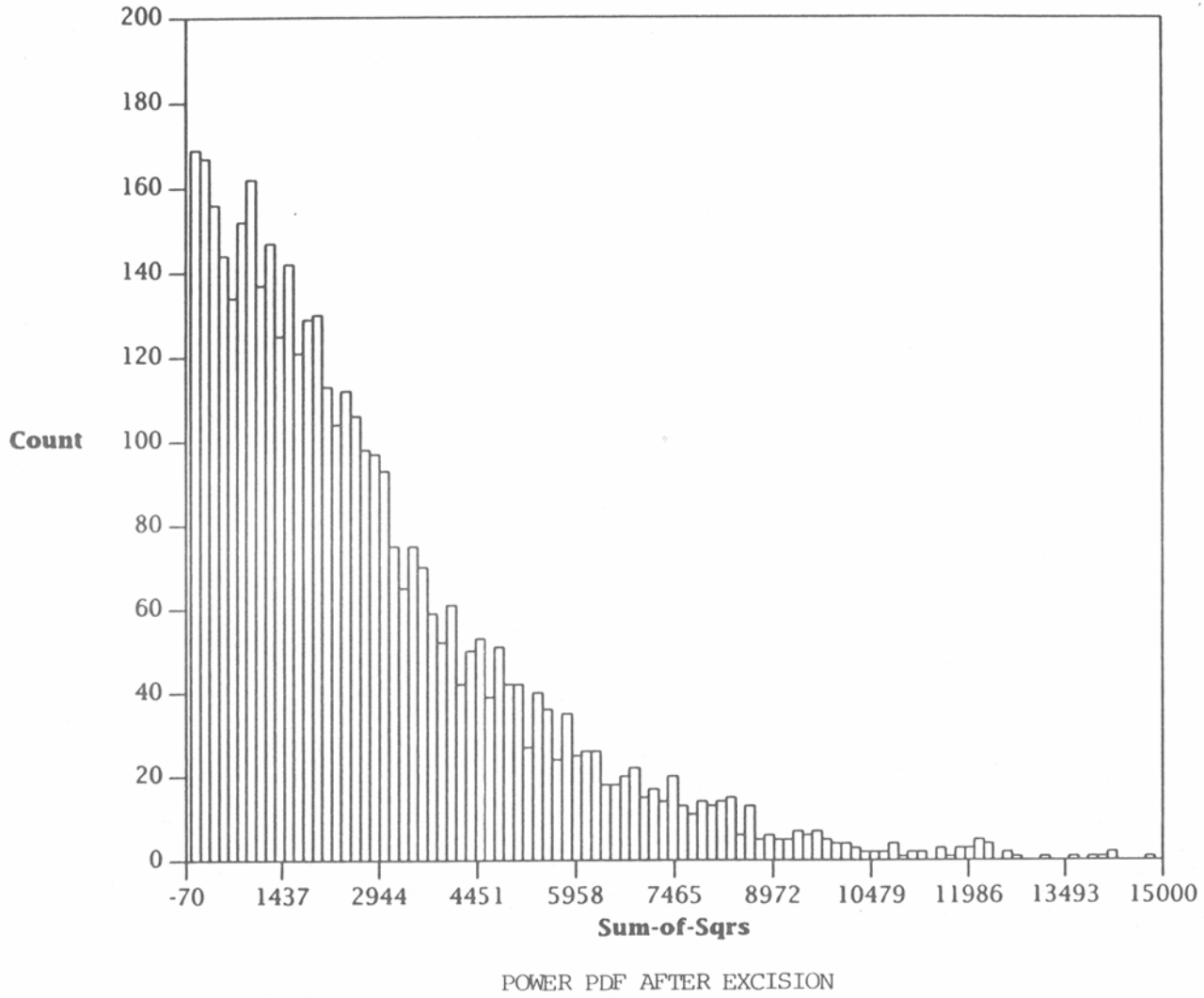

Figure 16. Probability density function of the power envelope in the time domain after excision of a single narrowband interferer (case study 2).

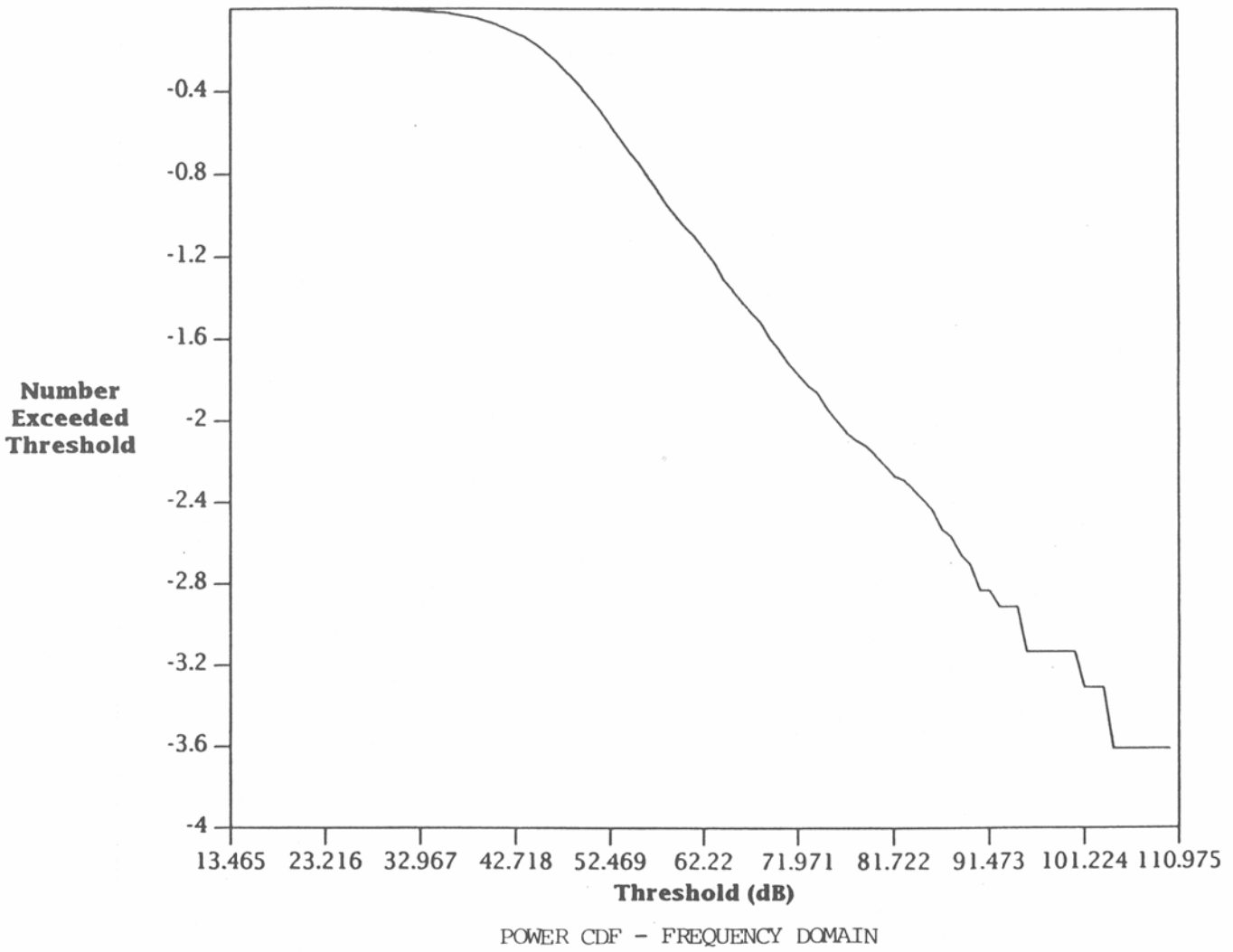

Figure 17. Cumulative distribution function of the power envelope in the frequency domain before excision (case study 2).

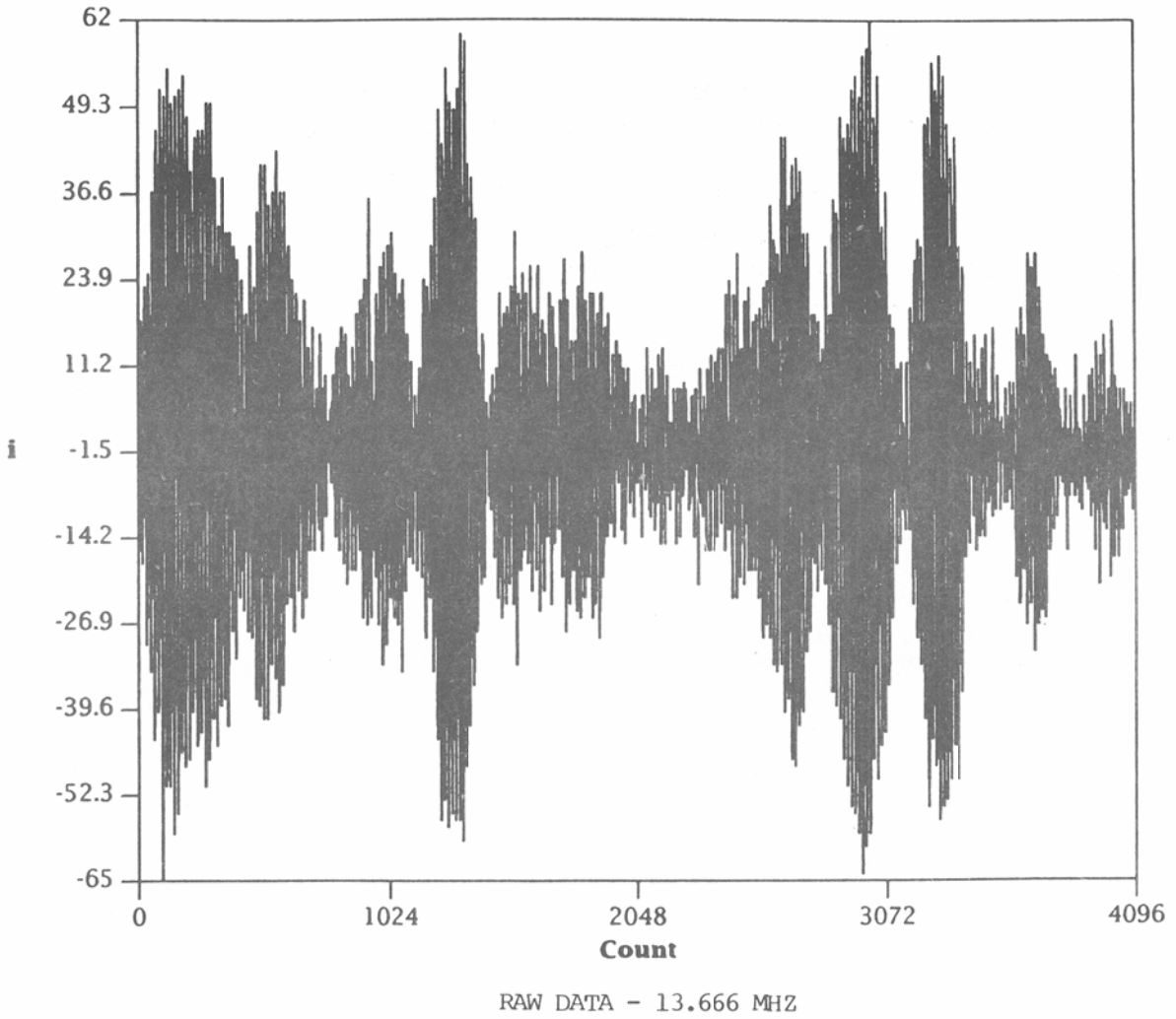

Figure 18. I-channel data at 13.666 MHz (case study 3).

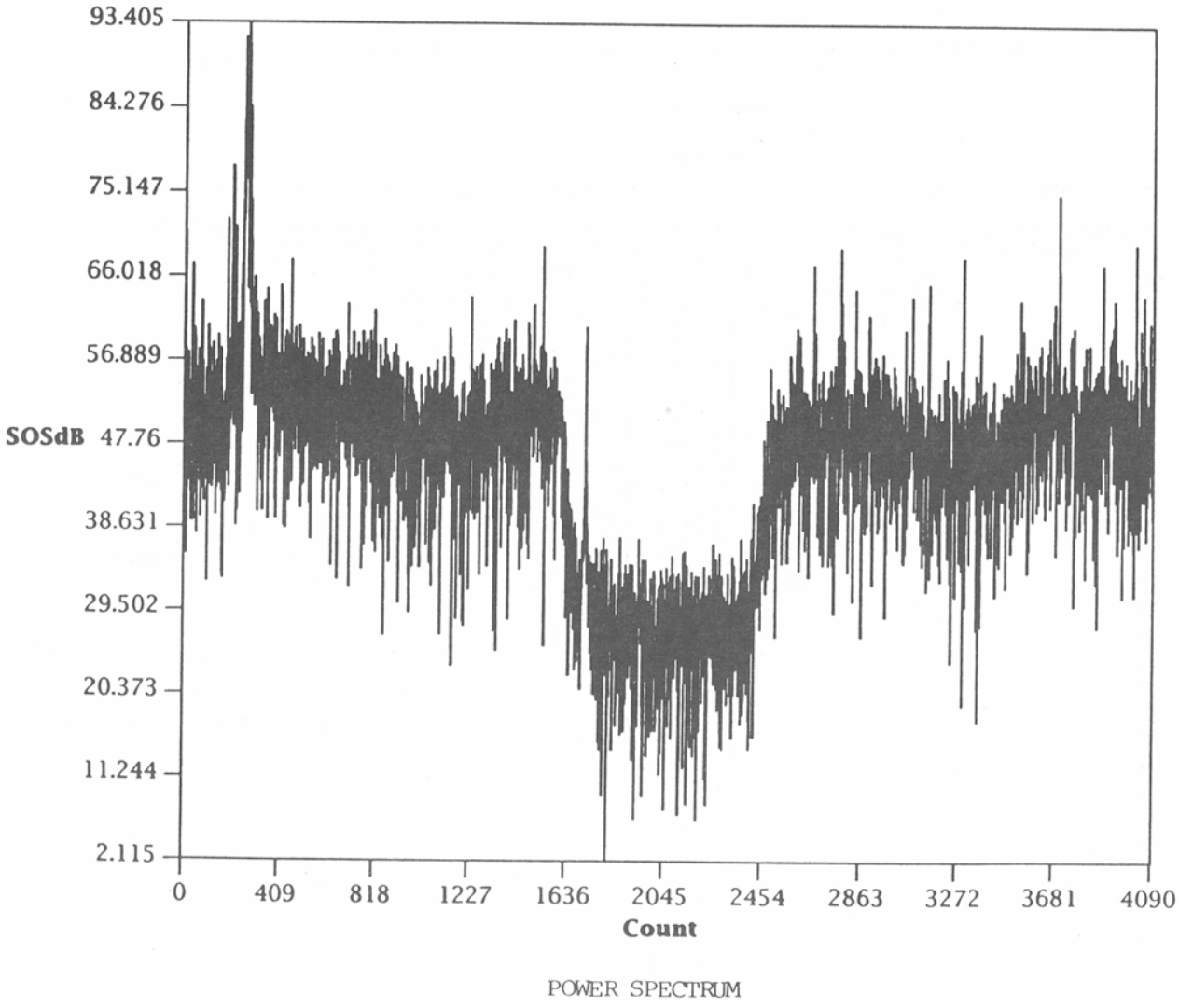

Figure 19. Power spectrum over a bandwidth of 1.024 MHz (case study 3).

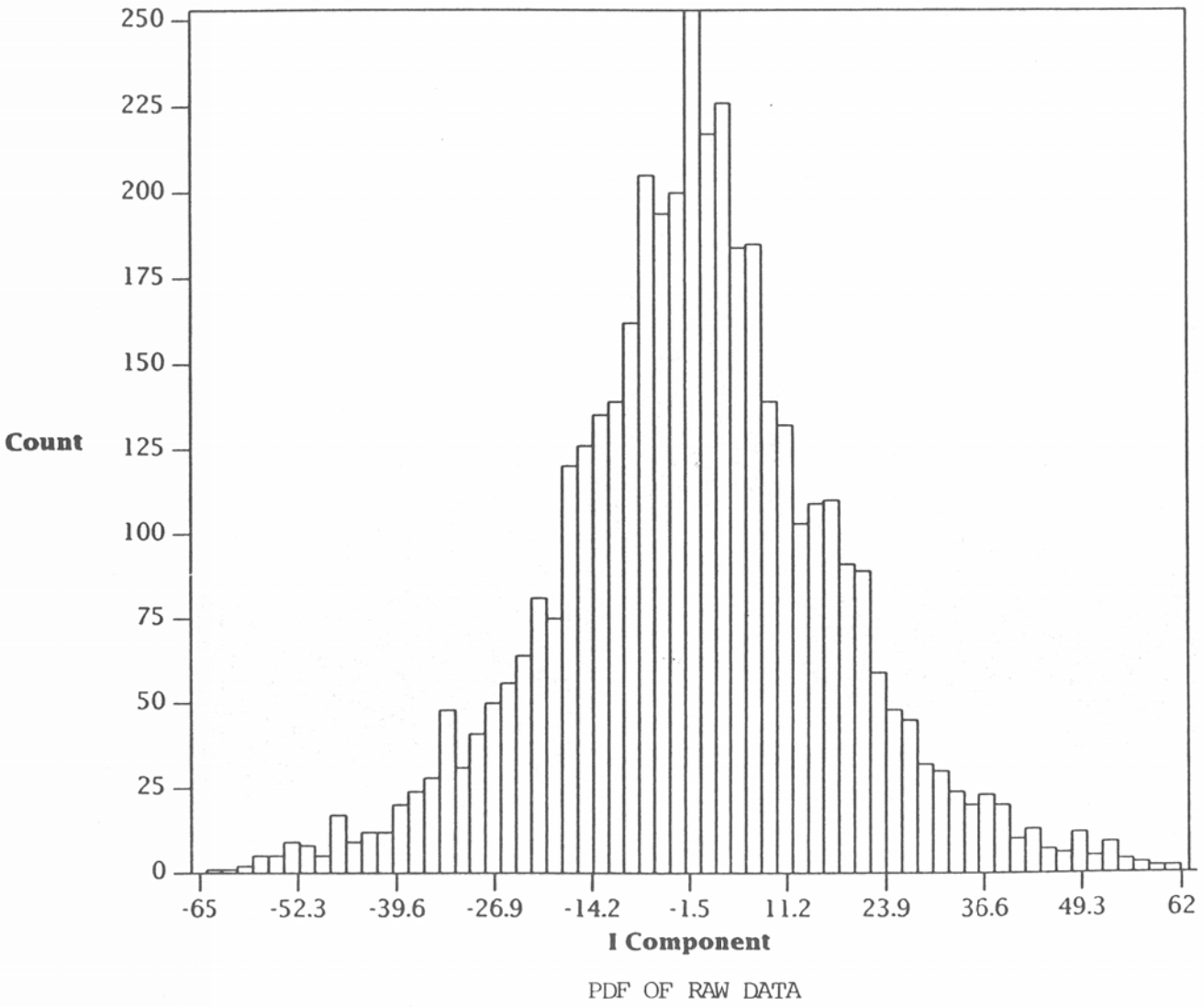

Figure 20. Probability density function of the I-channel data (case study 3).

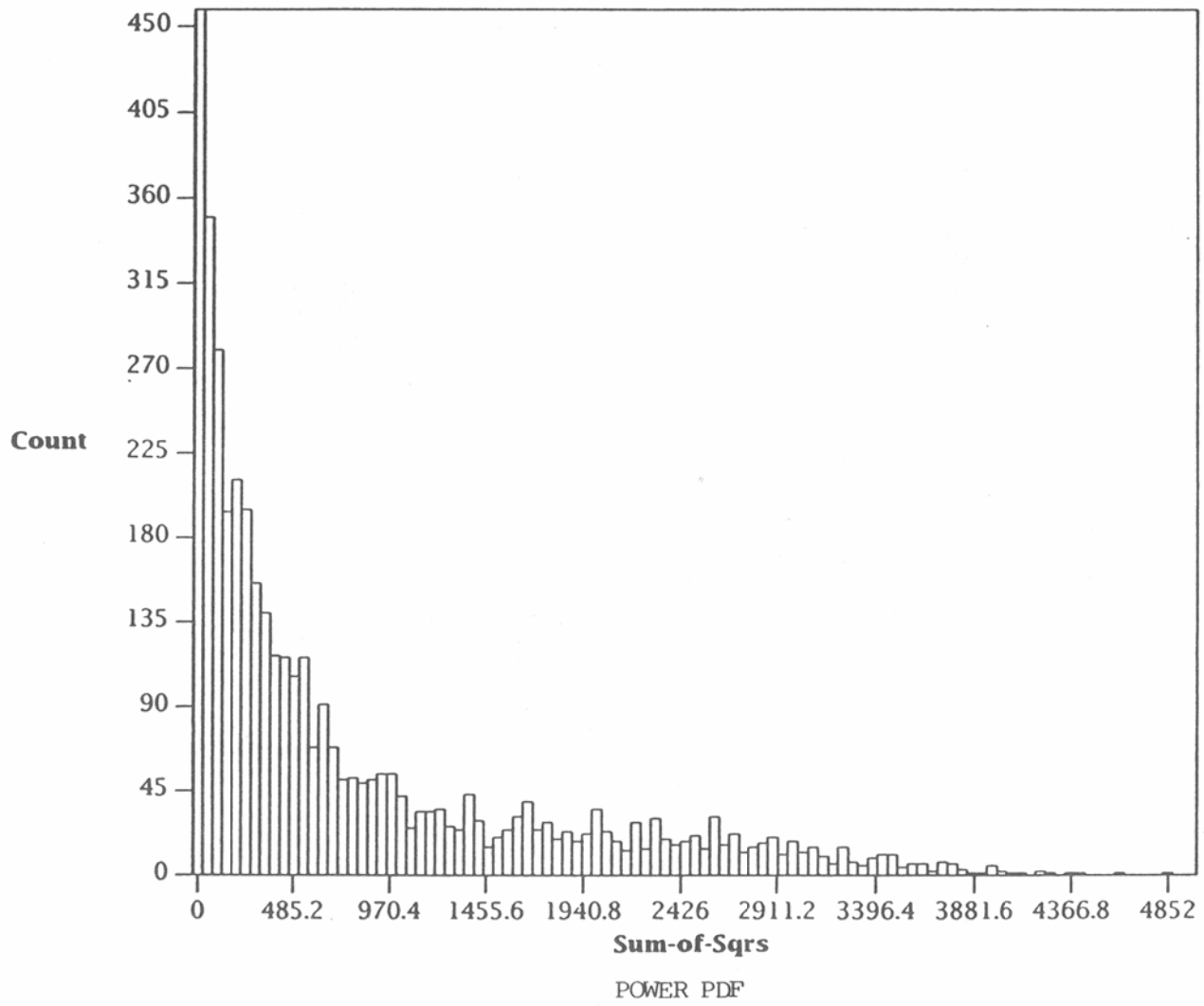

Figure 21. Probability density function of the power envelope in the time domain (case study 3).

distributions fall off exponentially). The existence of long tails is suggestive of an impulsive phenomenon; examples of this are discussed below. However, the cdf of the power envelope in the present case, shown in Figure 22, appears qualitatively similar to those of the previous cases. Thus, the appearance of the distributions in Figures 20 and 21 is presumably due to the strong envelope modulation in the raw data, and is not due to a truly impulsive process.

The cdf of the power envelope in the frequency domain is shown in Figure 23, and is also similar to those of previous cases, although the tail of the distribution is somewhat more pronounced. However, it will be shown in Section 3 that a combination of Gaussian noise and cw interferers whose amplitudes are distributed according to the Hall model can generate frequency domain cdfs which are quite similar to that in Figure 23, as well as those in the previous cases, depending on the values of the model parameters.

We conclude that once again the noise/interference can be viewed as a combination of a Gaussian process and many narrowband interferers.

2.3.4 Case Study 4.

The data in this case study were obtained at 02:31:33 UT on 29 March 1989, at a center frequency of 13.666 MHz. A plot of the first 4 ms of the I-channel data is shown in Figure 24. This case was selected because of the periodic oscillations in the data, which suggest that the noise/interference is dominated by a single strong narrowband interferer.

The pdf of the I-channel data is shown in Figure 25, and does indeed resemble the pdf for a single sine wave (recall that the pdf for the process $x=A \sin(\omega t)$ is $p(x) = 1/\pi\sqrt{(A^2-X^2)}$). The power spectrum is shown in Figure 26, and does reveal the presence of a single strong narrowband interferer whose power is more than 10 dB greater than that of any of the other interferers.

Nevertheless, it would be incorrect to conclude that the statistics of the noise/interference can be described by those of a single narrowband interferer. The power pdf's in both time and frequency for a single sine wave consist of delta functions, and the cdf's therefore consist of step functions. On the other hand, the cdf's of the power envelope

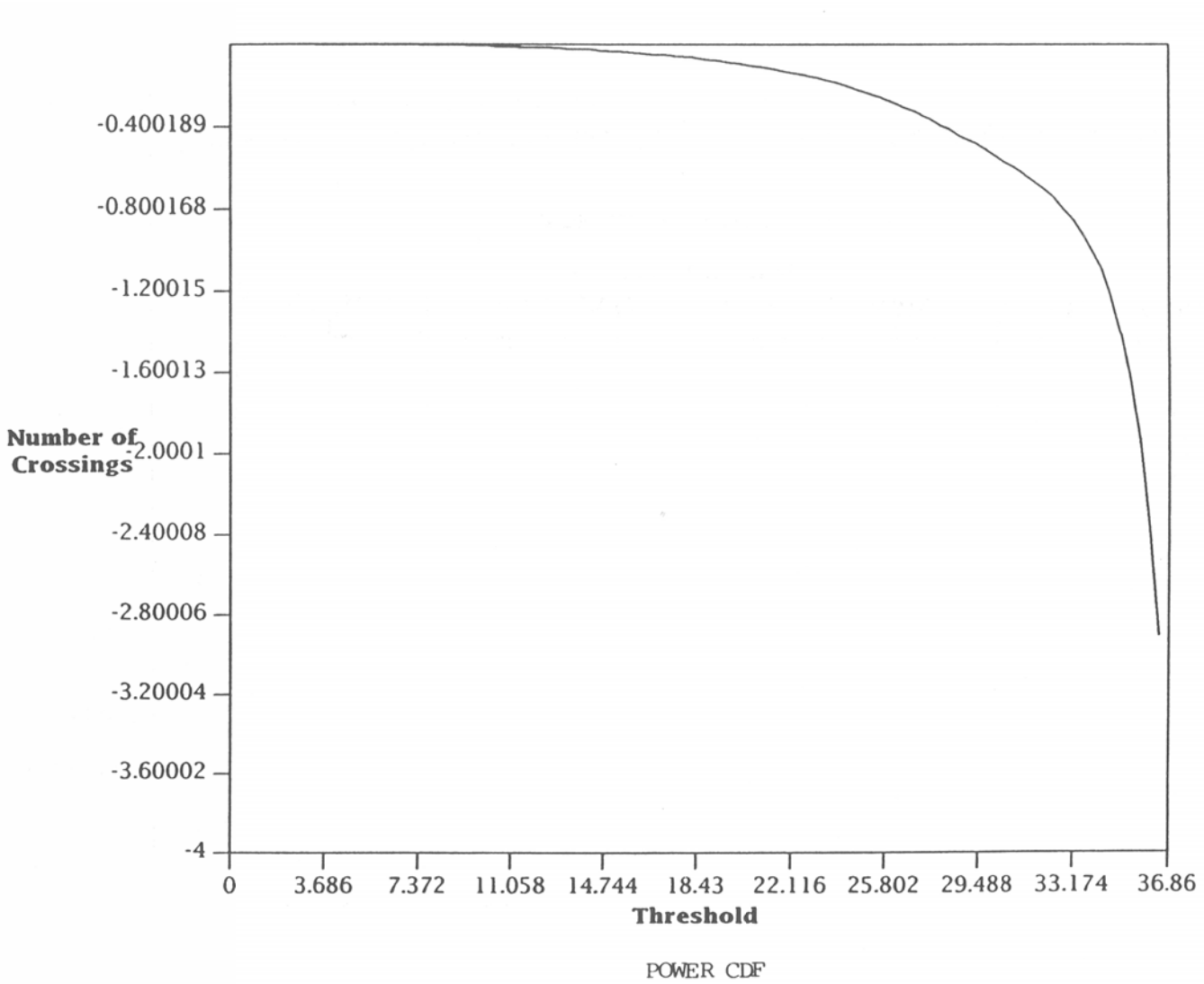

Figure 22. Cumulative distribution function of the power envelope in the time domain (case study 3).

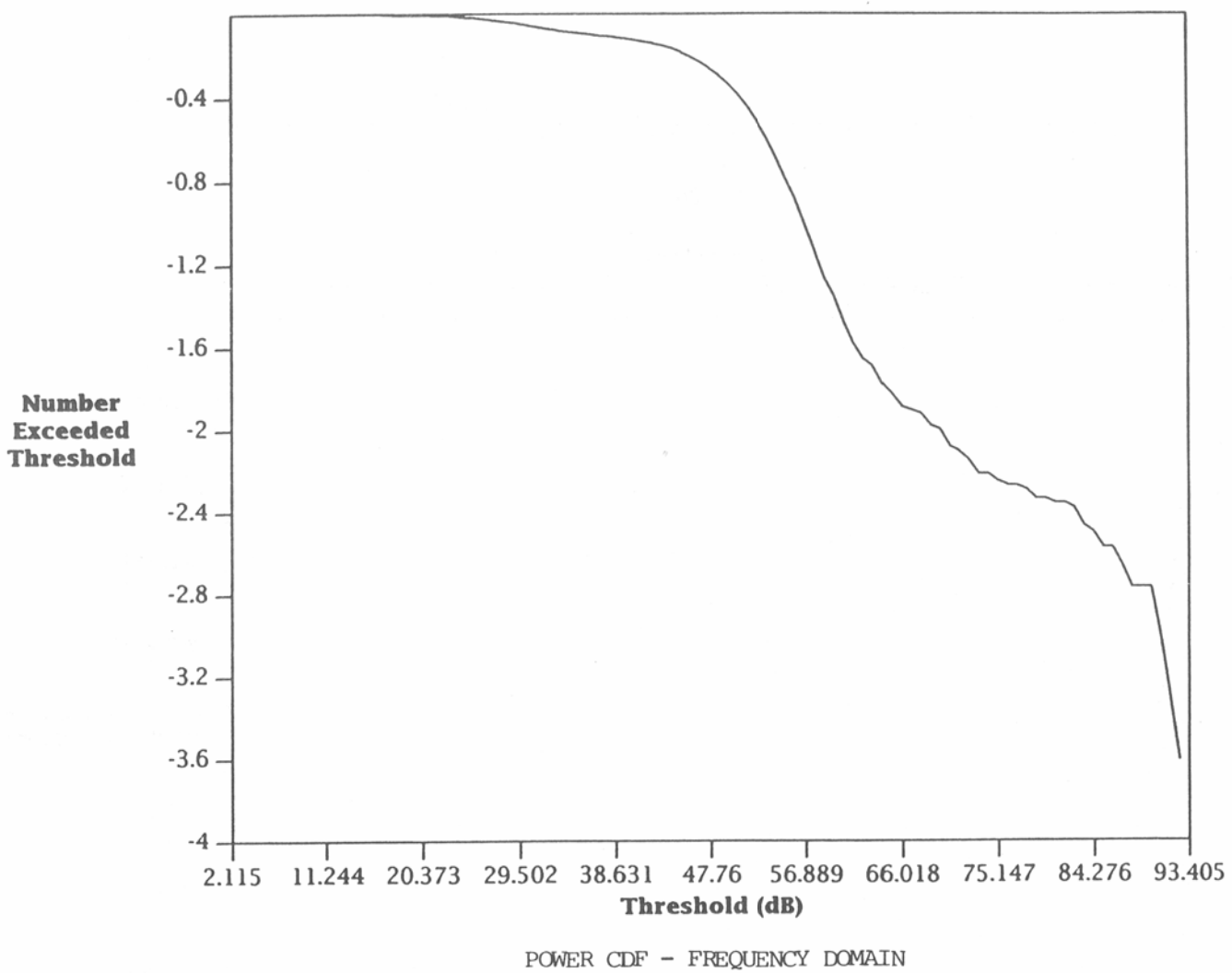

Figure 23. Cumulative distribution function of the power envelope in the frequency domain (case study 3).

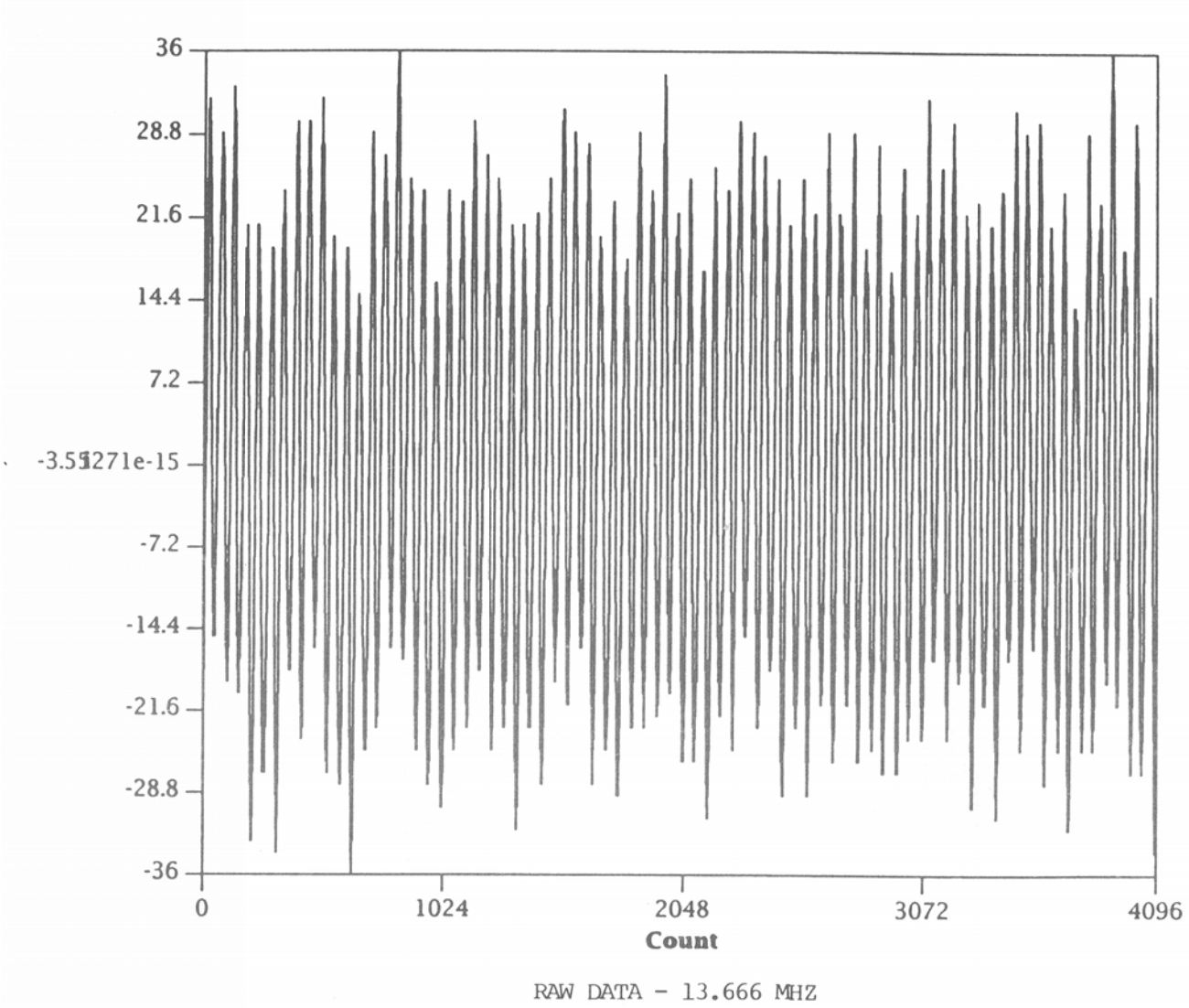

Figure 24. I-channel data at 13.666 MHz (case study 4).

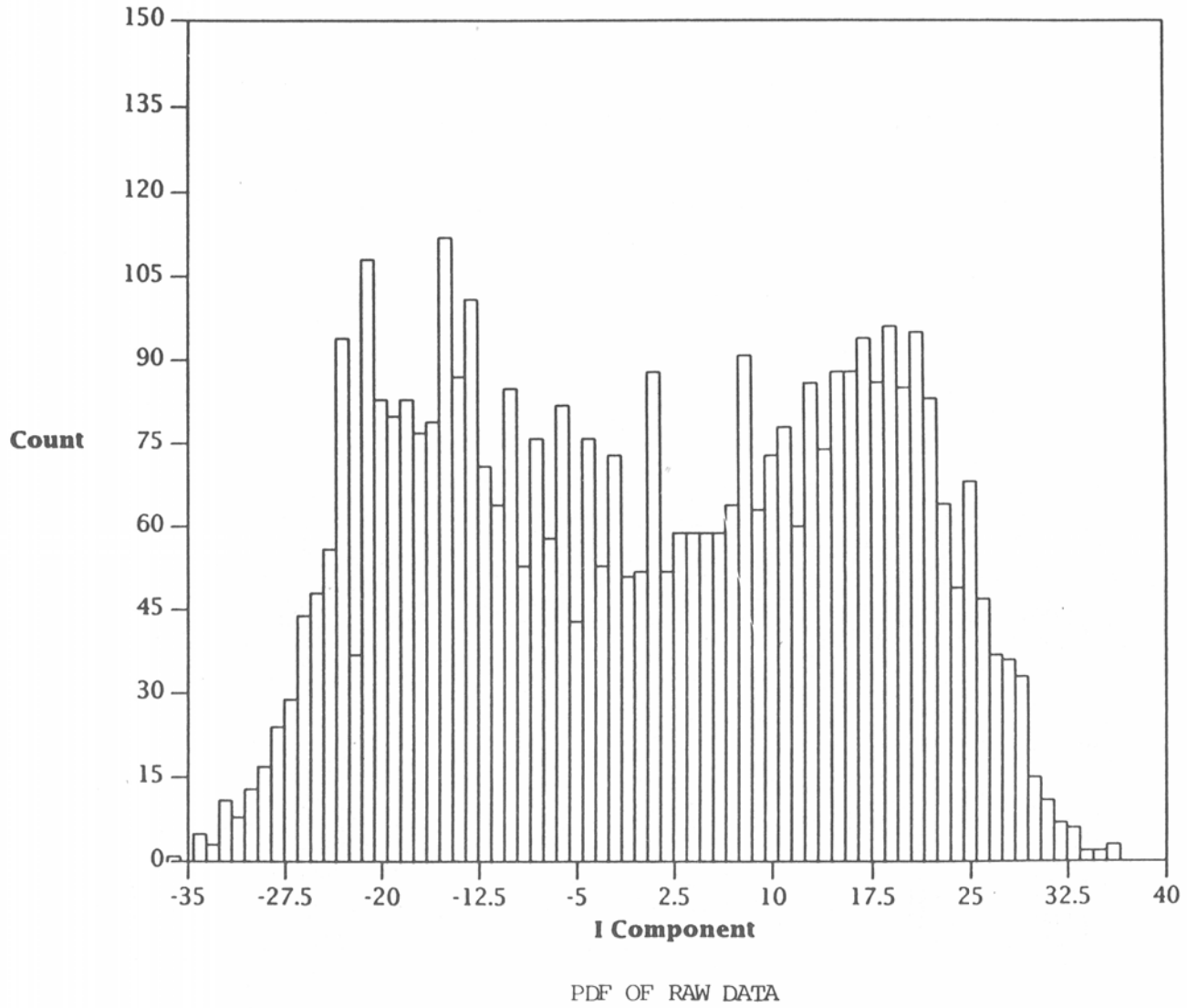

Figure 25. Probability density function of the I-channel data (case study 4).

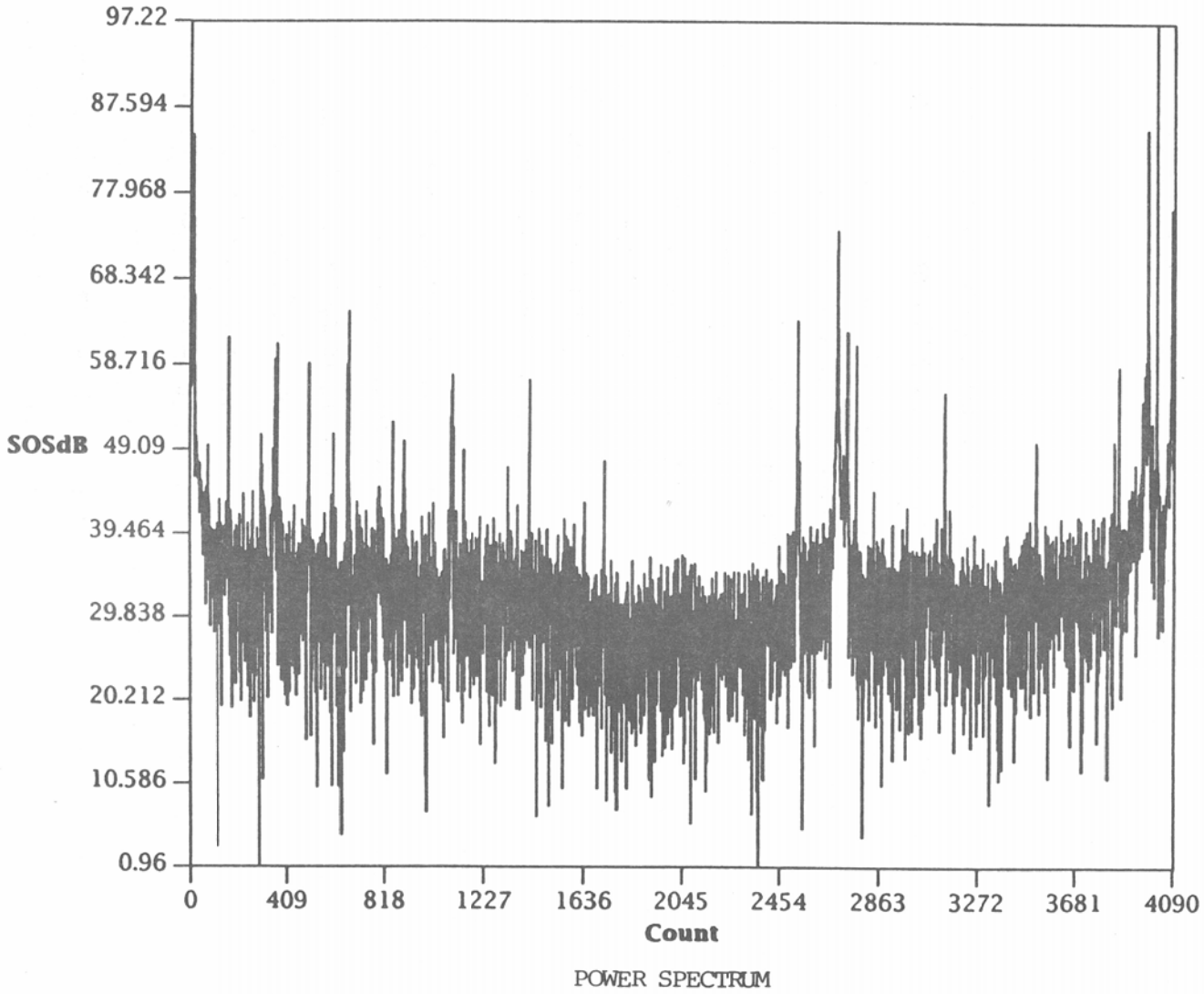

Figure 26. Power spectrum over a bandwidth of 1.024 MHz (case study 4).

of the noise/interference in the time and frequency domains are shown in Figures 27 and 28, respectively. These cdf's are clearly not step functions, and in fact resemble the cdf's of the previous case studies. In modeling the noise/interference it is therefore important to take into account the presence of the many narrowband interferers and the Gaussian noise even though the noise/interference power is dominated by a single interferer.

2.3.5 Case Study 5.

The data in this case study were obtained at 19:22:31 UT on 15 March 1989 at a center frequency of 23.862 MHz. A plot of the first 4 ms of the I-channel data is shown in Figure 29. This case was selected because of the impulsive nature of the noise. Of the 42 noise records examined in this study, this noise record is the only one that clearly exhibits impulsive noise in the raw data. The origin of the noise pulses is unknown, but is almost certainly not atmospheric noise. The reason is because the noise pulses do not occur randomly in time, but appear to occur in a quasi-periodic fashion. For example, Figure 30 shows 4 ms of the I-channel data from another part of the I-second noise record (not the first 4 ms shown in Figure 29). The noise pulses are not precisely periodic in time, but tend to be separated by approximately .5 ms; thus, the source of the impulses has been assumed to be of manmade origin.

In this particular noise record the quantization of the noise samples is apparent from inspection of Figures 29 and 30. The reason is presumably because the gain of the HF receiver was decreased to prevent the noise impulses from saturating the system, so that the voltage level of the noise floor was comparable to the resolution of the A/D converters.

The pdf's of the I-channel data and the power envelope for the first 4 ms of the noise record are shown in Figures 31 and 32, respectively. These results appear qualitatively similar to those of the previous case studies, except for the appearance of long tails in the distributions at high voltage (power) levels, which are the hallmark of an impulsive process. The tail in the power distribution is more readily apparent in the power cdf plotted on logarithmic scales, shown in Figure 33.

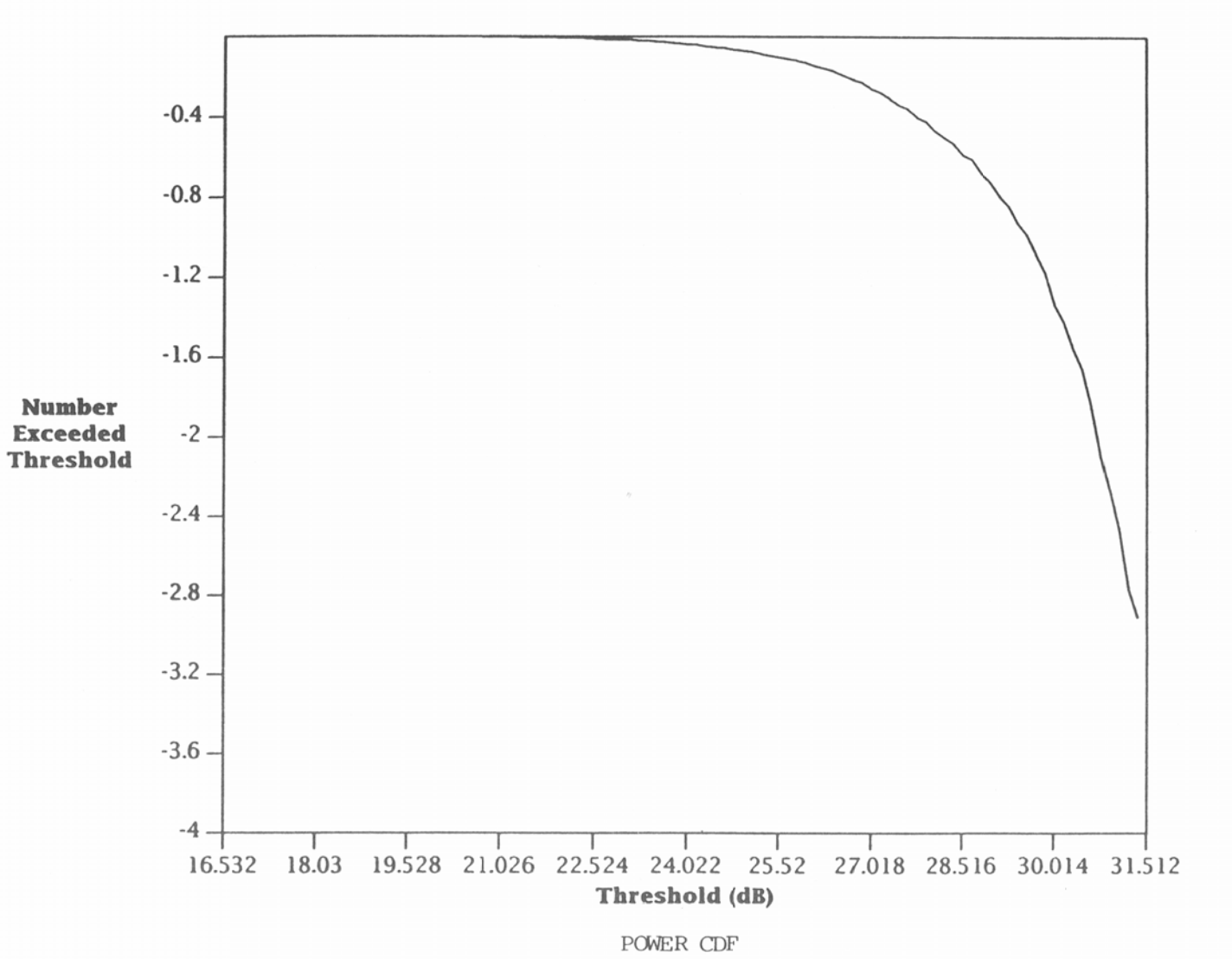

Figure 27. Cumulative distribution function of the power envelope in the time domain (case study 4).

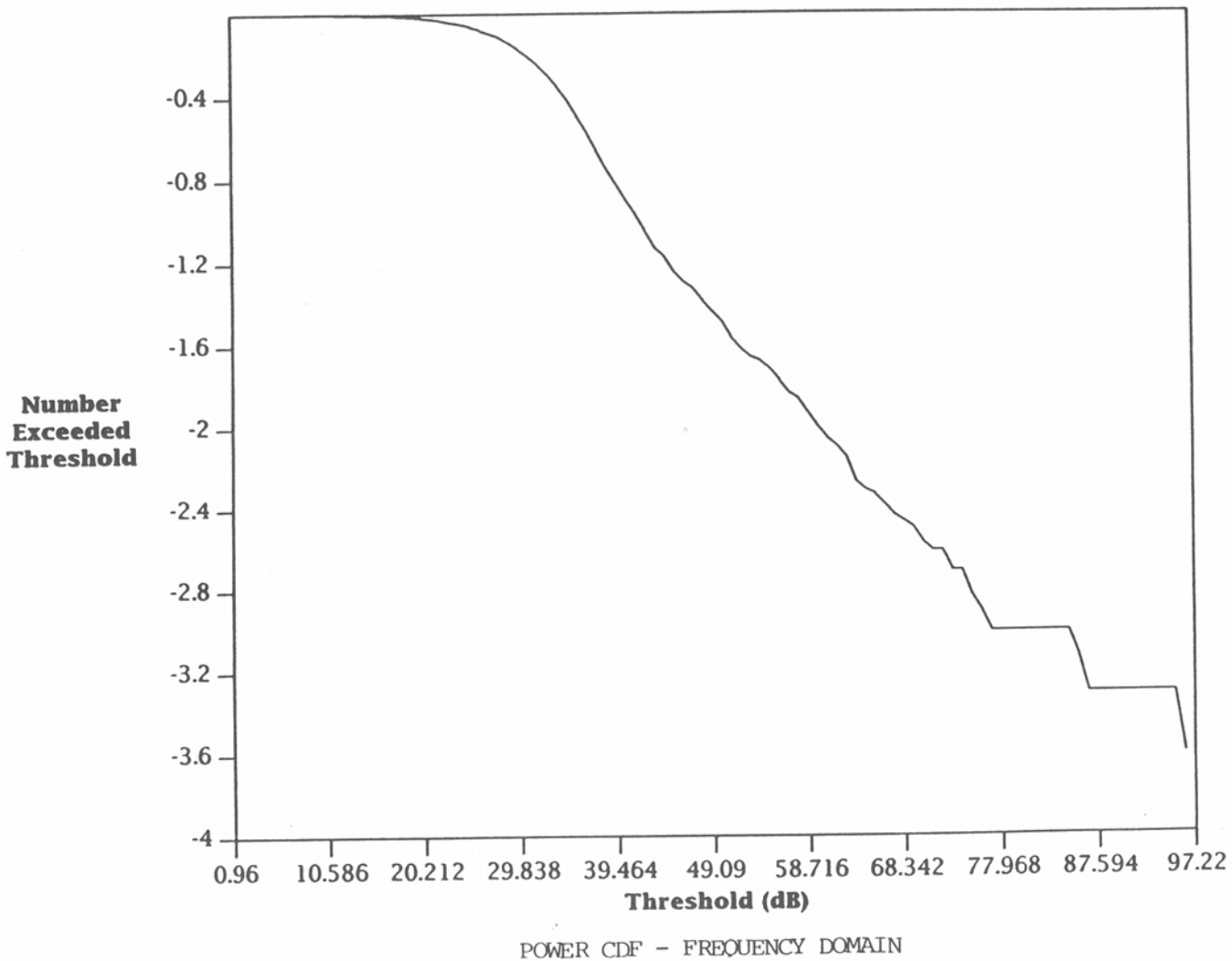

Figure 28. Cumulative distribution function of the power envelope in the frequency domain (case study 4).

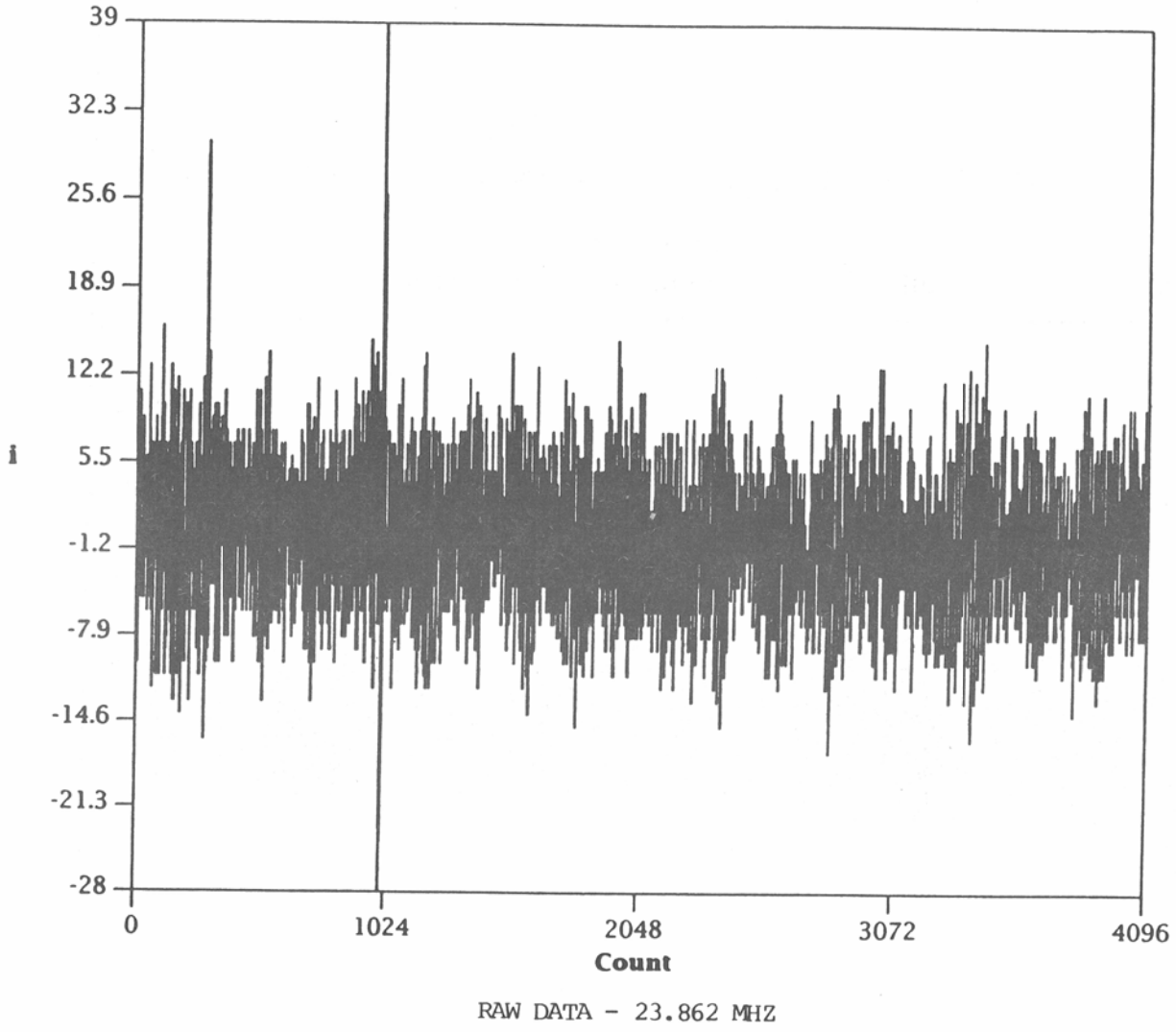

Figure 29. I-channel data at 23.862 MHz (case study 5).

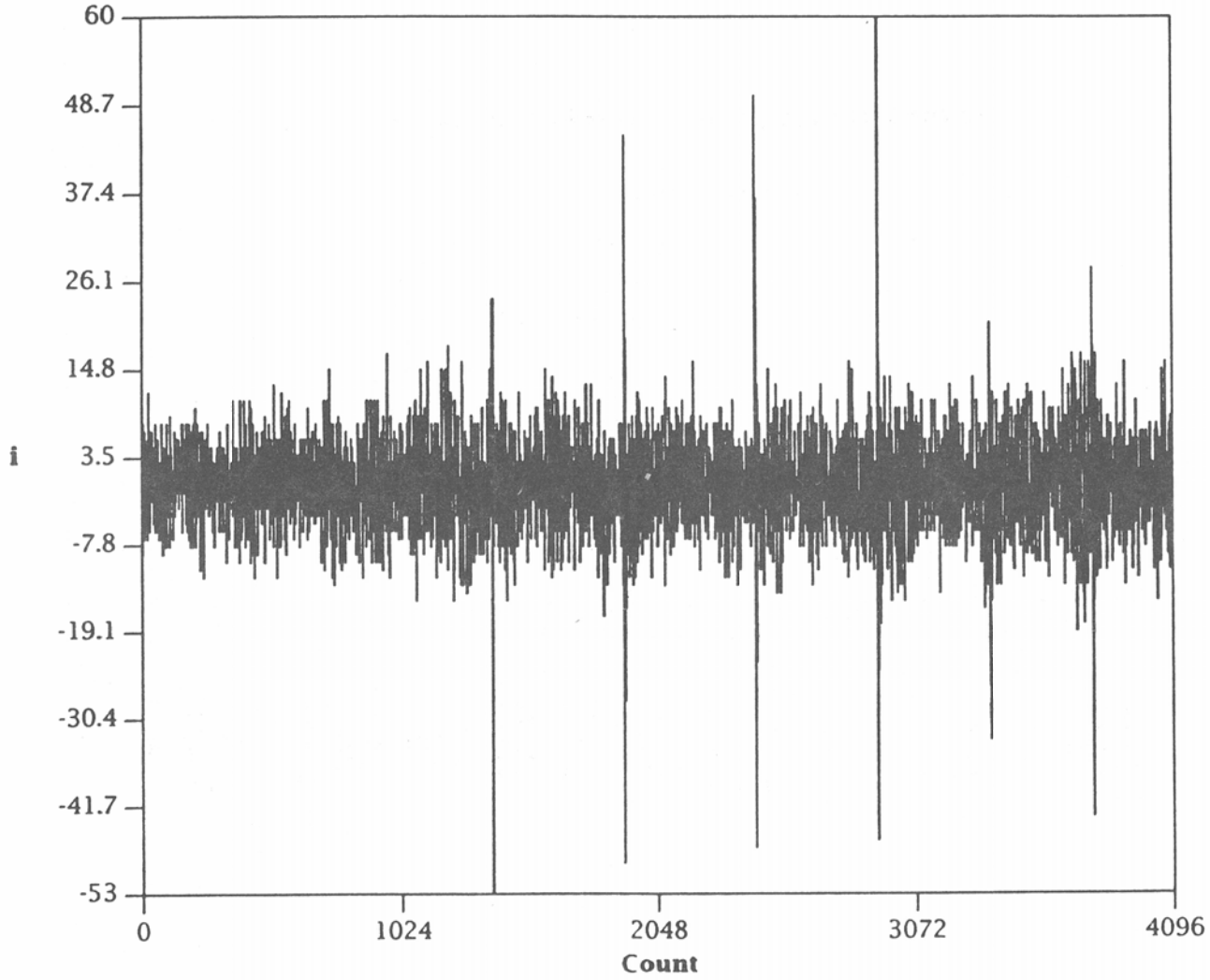

Figure 30. I-channel data at 23.862 MHz (case study 5).

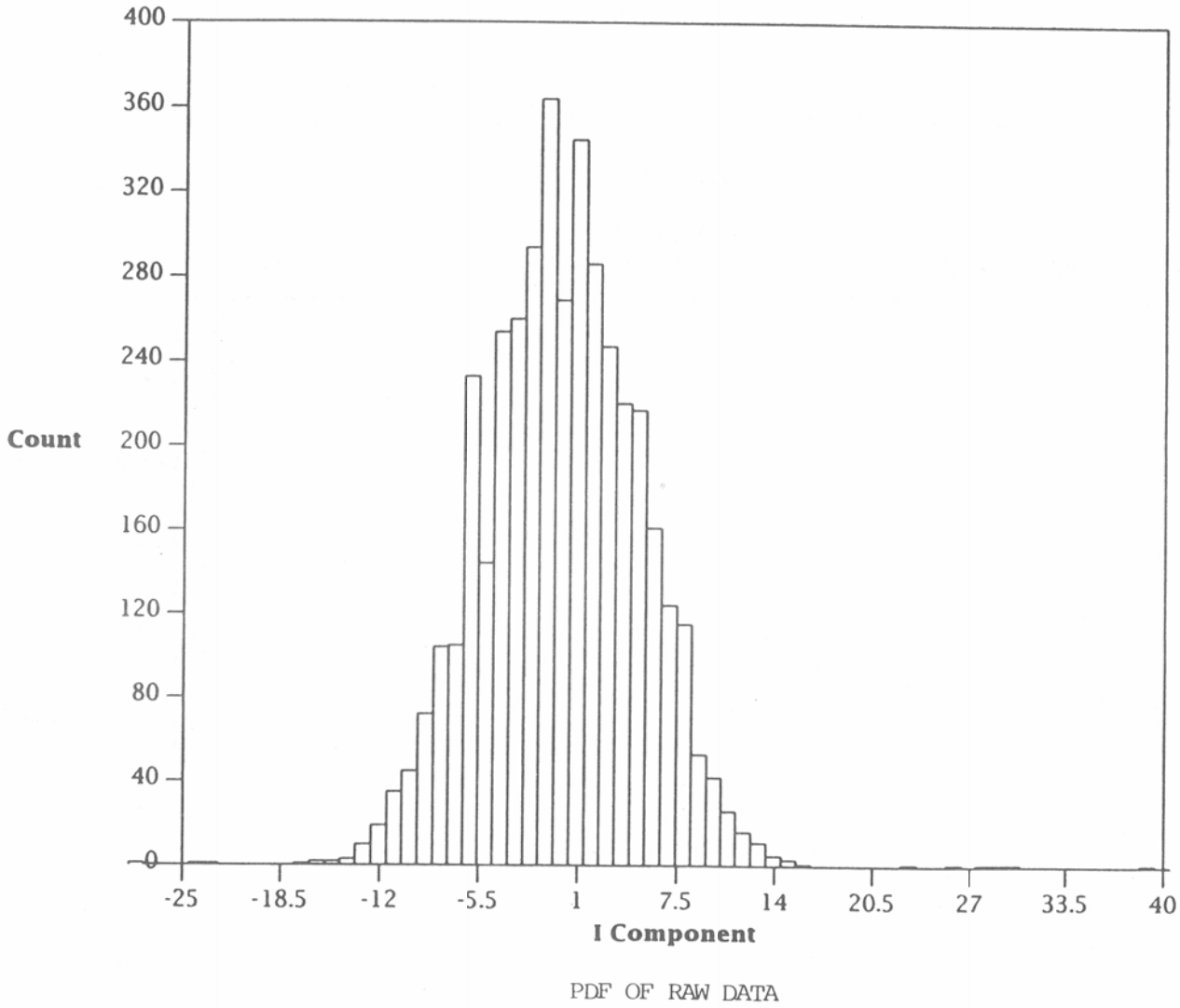

Figure 31. Probability density function of the I-channel data (case study 5).

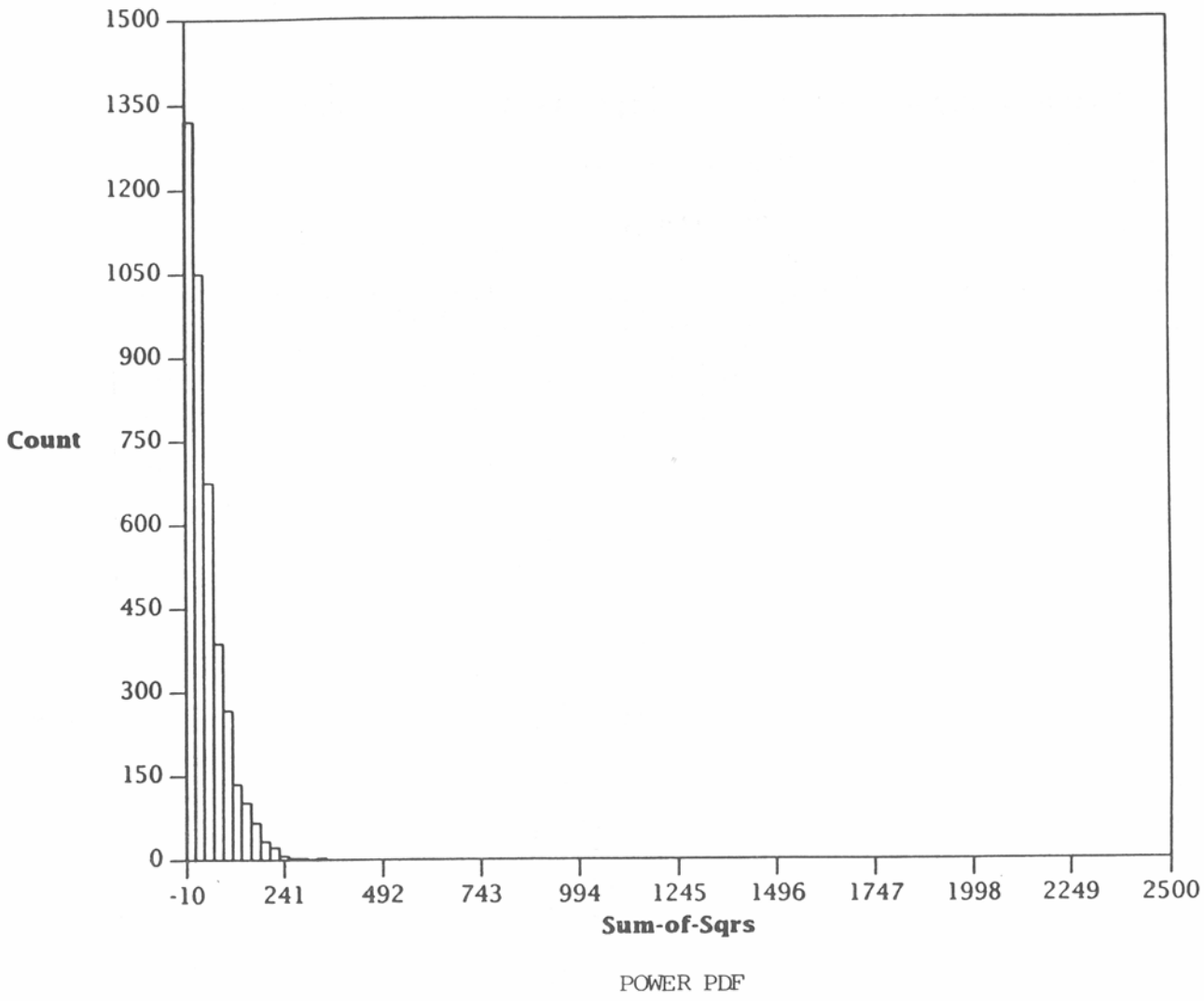

Figure 32. Probability density function of the power envelope in the time domain (case study 5).

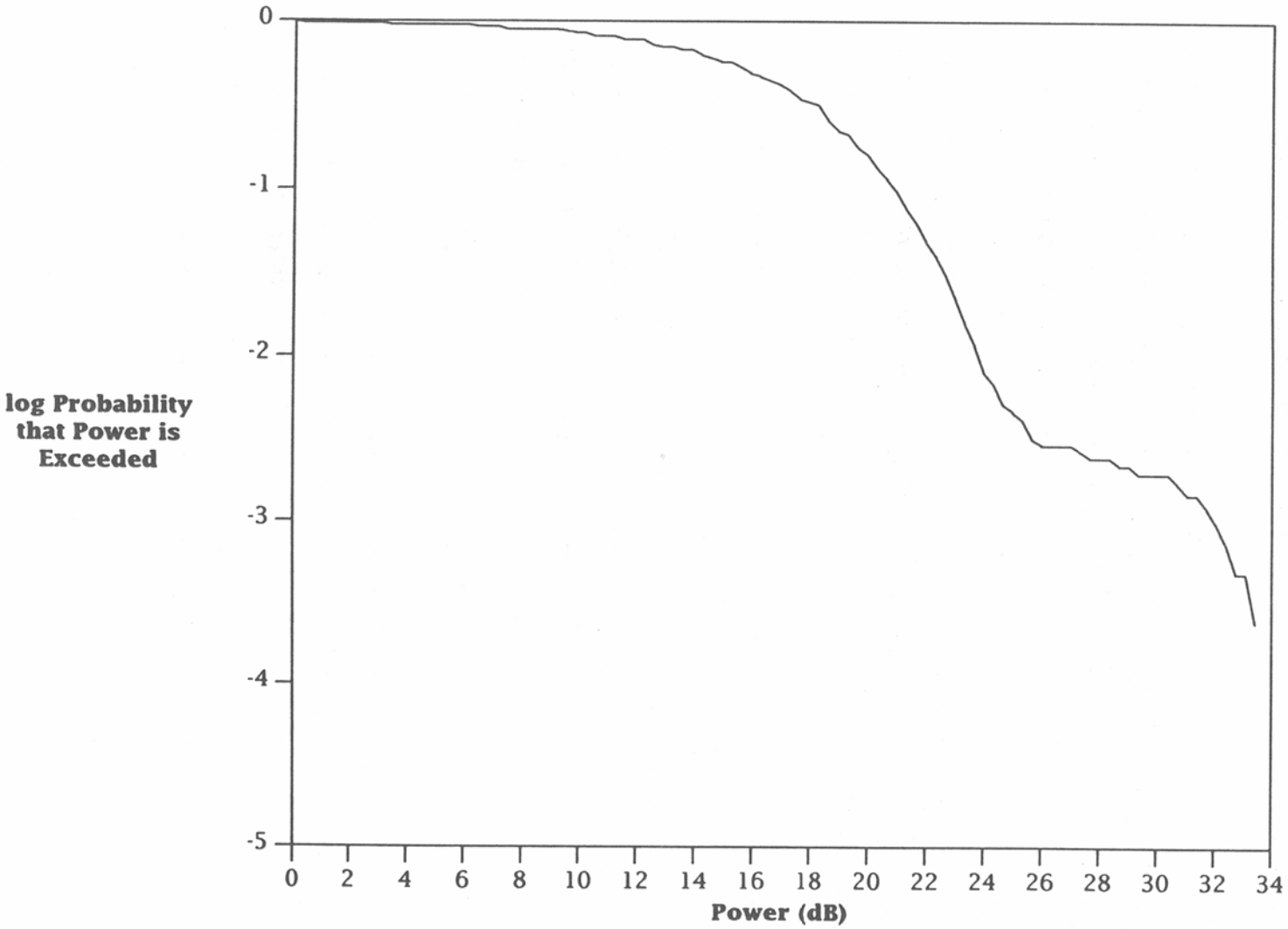

Figure 33. Cumulative distribution function of the power envelope in the time domain (case study 5).

The level crossing distribution of the voltage envelope is shown in Figure 34. Again, this distribution is similar to those of previous cases (see, for example, Figure 7), except for the long tail at high voltage levels.

The presence of impulsive noise is also apparent in the power spectrum, shown in Figure 35. The fact that the noise floor within the 400 kHz bandpass of the filters in the HF receiver is greater (by approximately 20 dB) than the noise floor outside the bandpass of the filters indicates that a broadband process (impulsive noise) is contributing to the power spectral density within the band.

The power spectrum also reveals the presence of numerous narrowband interferers, as in previous cases. The power distribution of these interferers can be obtained from the power cdf in the frequency domain, plotted in Figure 36, which is again similar to those of previous cases.

Because the data in this case study clearly reveal the presence of impulsive noise, which is not apparent in the previous cases, it is of interest to see what effect, if any, the impulsive noise has on the phase distributions. The pdf's of the phase in both the time and frequency domains are shown in Figures 37 and 38, respectively. Unlike the previous time domain phase distributions, which are uniform, the distribution in Figure 37 is clearly nonuniform, with spikes occurring at discrete values of phase. On the other hand, the frequency domain phase distribution in Figure 38 is qualitatively similar to those of the previous cases.

The peculiar spikes in the time domain phase distribution can be understood as an artifact which arises due to the aforementioned quantization of the raw data. Because the I- and Q-channel voltages are integral multiples of a fundamental voltage (the resolution of the A/D converters), it follows that the phase is discretized at values equal to the arctangent of the ratio of two integers. Thus, one expects peaks in the phase distribution at $\arctan(0/1)=0$, $\arctan(1/0)=\pi/2$, $\arctan(1/1)=\pi/4$, $\arctan(1/2)=0.46$, etc., and peaks at precisely these values of phase can be seen in Figure 37.

To summarize, it appears that the noise/interference in this case study can be described by a combination of Gaussian noise, narrowband interferers, and impulsive noise.

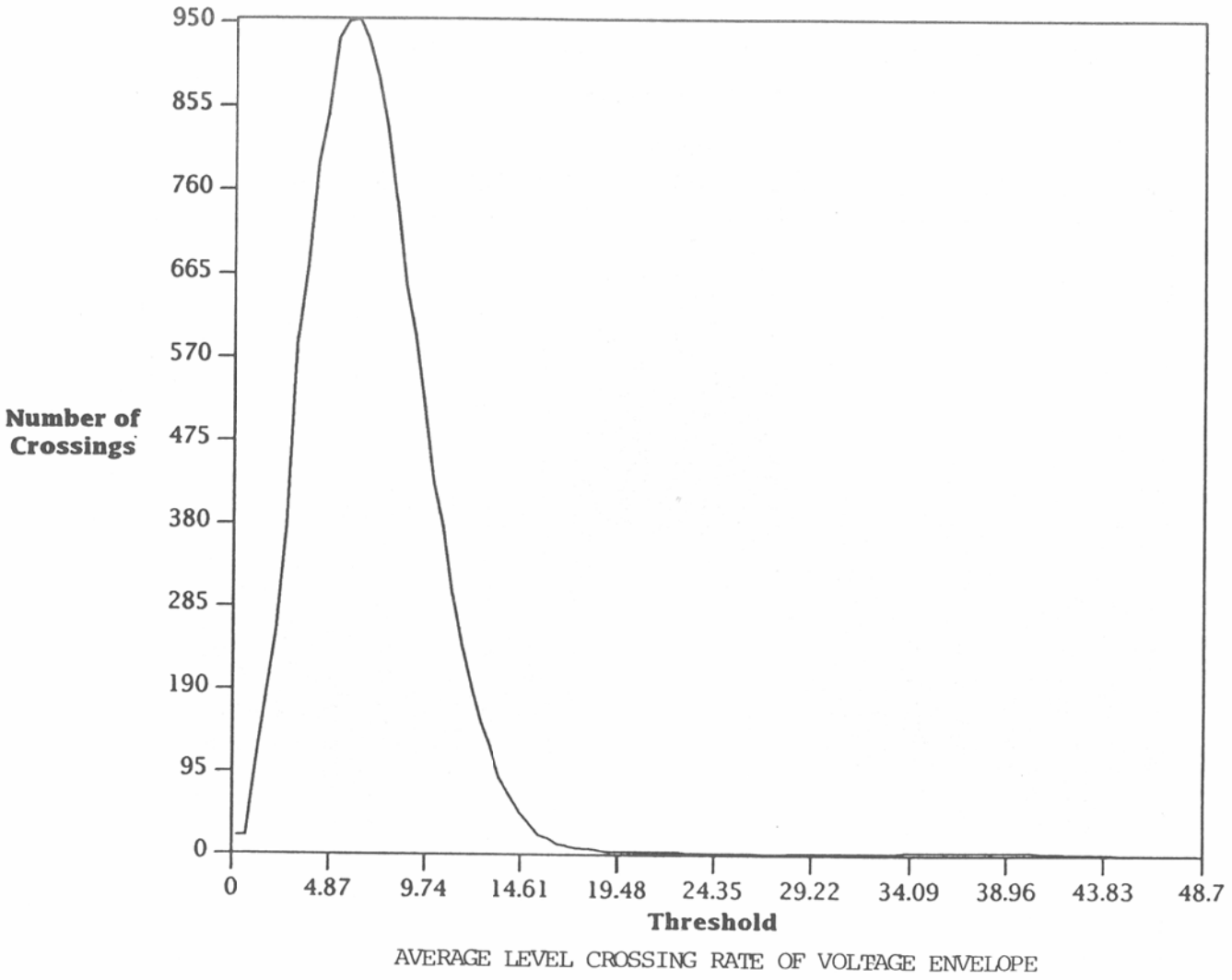

Figure 34. Level crossing distribution of the voltage envelope (case study 5).

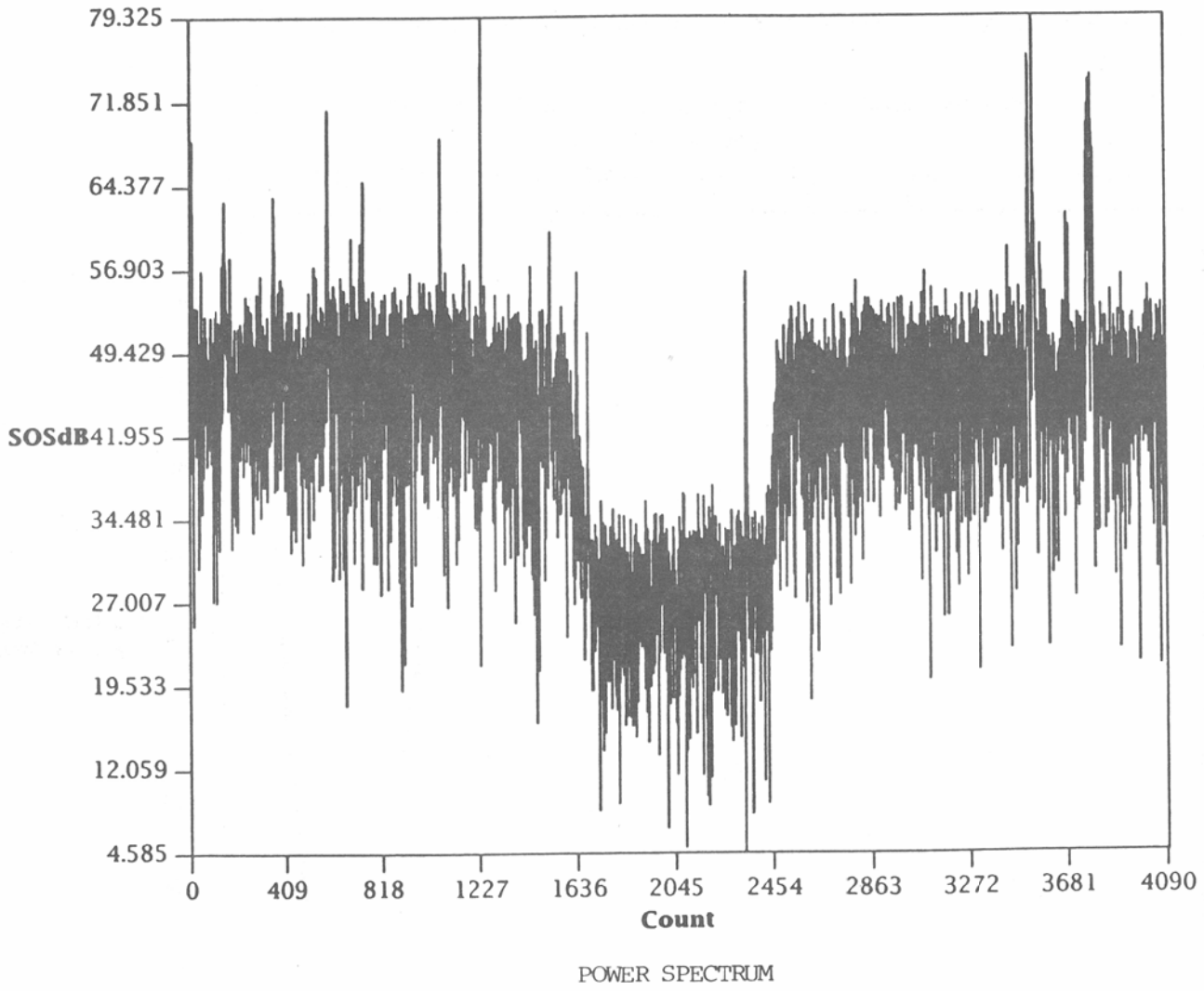

Figure 35. Power spectrum over a bandwidth of 1.024 MHz (case study 5).

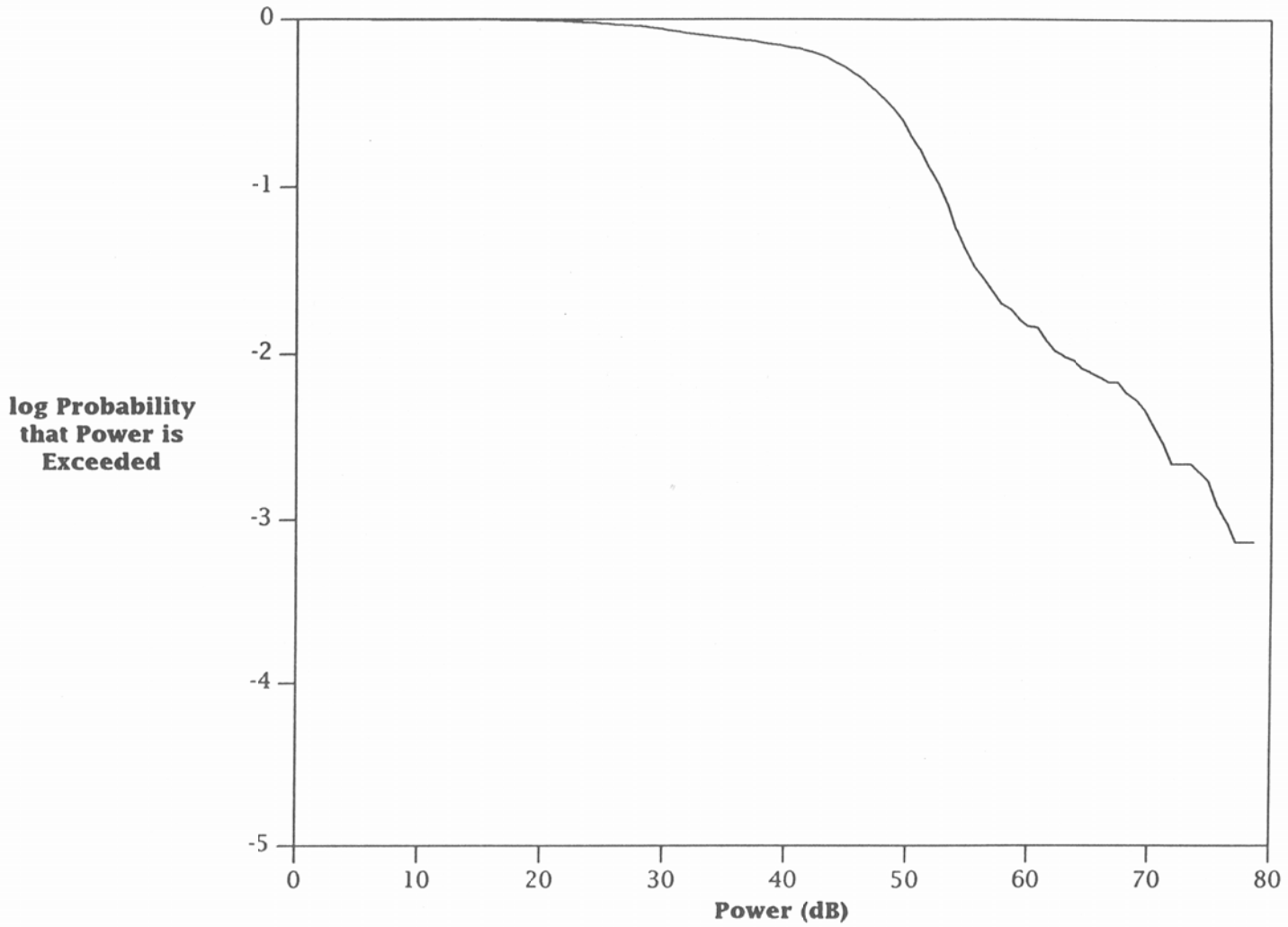

Figure 36. Cumulative distribution function of the power envelope in the frequency domain (case study 5).

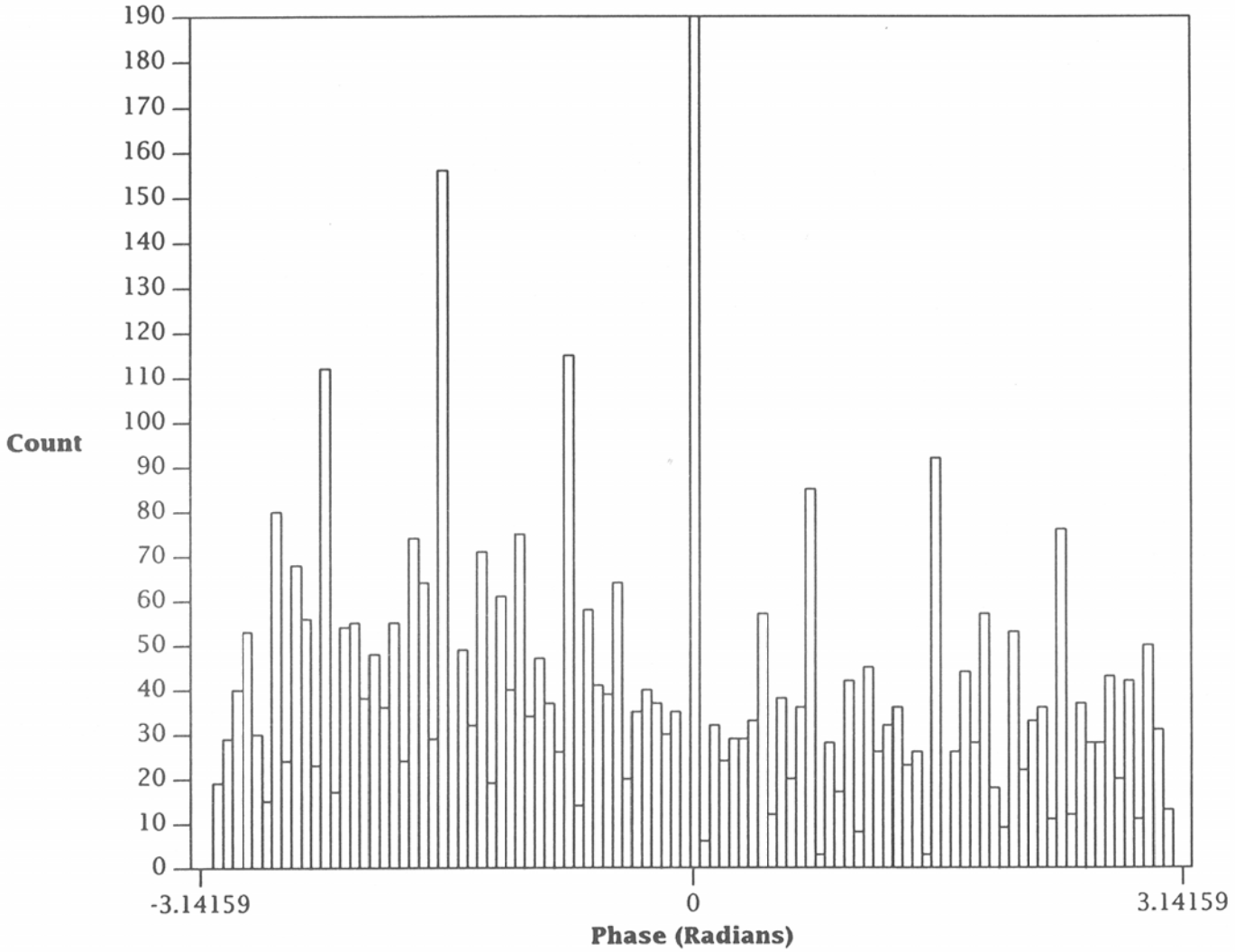

Figure 37. Probability density function of the phase in the time domain (case study 5).

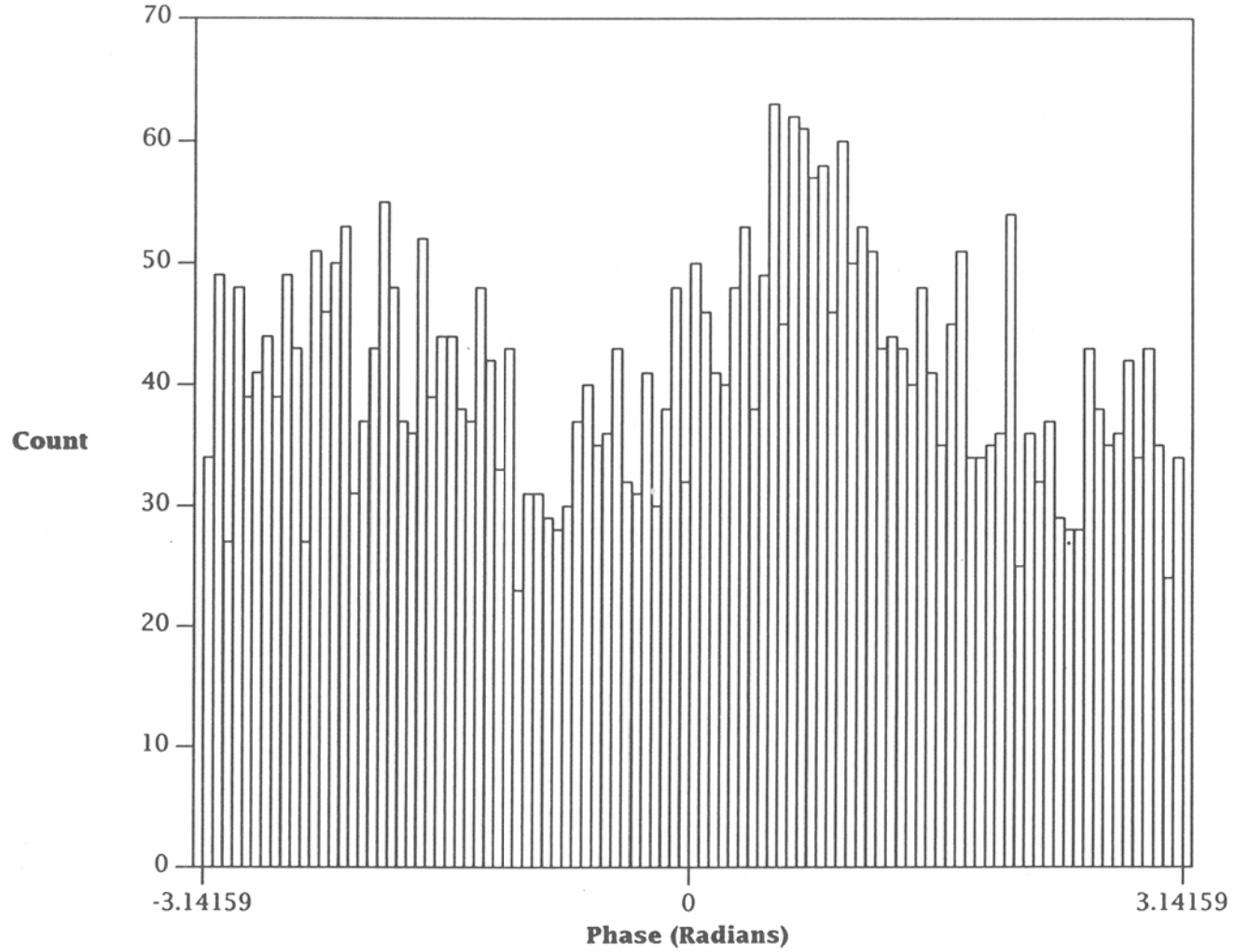

Figure 38. Probability density function of the phase in the frequency domain (case study 5).

The Gaussian noise and narrowband interferers have statistical properties similar to those of the previous cases. The impulsive noise must be modeled by a process which yields the aforementioned tails in the amplitude and crossing rate distributions, but not the spikes in the time domain phase distribution, which are an artifact of the A/D conversion.